Comparing Predictive Accuracy in the Presence of a Loss Function Shape Parameter*

Sander Barendse — Oxford University
Andrew J. Patton — Duke University

May 28, 2019

Abstract

We develop tests for out-of-sample forecast comparisons based on loss functions that contain shape parameters. Examples include comparisons using average utility across a range of values for the level of risk aversion, comparisons of forecast accuracy using characteristics of a portfolio return across a range of values for the portfolio weight vector, and comparisons using recently-proposed "Murphy diagrams" for classes of consistent scoring rules. An extensive Monte Carlo study verifies that our tests have good size and power properties in realistic sample sizes, particularly when compared with existing methods which break down when then number of values considered for the shape parameter grows. We present three empirical illustrations of the new test.

Keywords: Forecasting, model selection, out-of-sample testing, nuisance parameters.

J.E.L. codes: C53, C52, C12.

*We thank Dick van Dijk, Erik Kole, Chen Zhou, and seminar participants at Oxford University for valuable discussions and feedback. The first author also acknowledges financial support from the Erasmus Trustfonds. All errors remain our own. Correspondence to: Sander Barendse, Nuffield College, New Road, Oxford, UK. Email address: sander.barendse@economics.ox.ac.uk.

1 Introduction

Forecast comparison problems in economics and finance invariably rely on a loss function or utility function, and in many cases these functions contain a shape parameter, for example, when comparing two forecasting models based on average utility. In many cases, there is no single specific value for the shape parameter that is of interest, rather there is a *range* of values that are of interest to the researcher. In this case the null hypothesis of equal predictive accuracy has a continuum of testable implications, but most existing work instead tests equal predictive accuracy at a few ad hoc values of the shape parameter. This paper builds on existing work on forecast comparison tests, see Diebold and Mariano (1995) and Giacomini and White (2006), with bootstrap theory for empirical processes, see Bühlmann (1995), to provide forecast comparison tests that allow for inference across a range of values of a loss function shape parameter.

A leading example of an application that depends on some arbitrary parameter is a test of equal expected utility in which the utility function is parameterized by a risk aversion parameter. Given that economists have not converged on what value of risk aversion is appropriate (see, e.g., Bliss and Panigirtzoglou (2004) for a discussion) it is desirable to consider a null hypothesis of equal expected utility over a range of reasonable risk aversion values, instead of testing at some single value. Current practice usually evaluates the hypothesis of equal expected utility at one or a select few risk aversion parameter values, see, for example, Fleming et al. (2001, 2003); Marquering and Verbeek (2004); Engle and Colacito (2006); and DeMiguel et al. (2007).

Another application that involves a continuum of testable implications is when one evaluates forecasts from multivariate models on the basis of their implied forecasts of univariate quantities, for example, evaluating a multivariate volatility model through its forecasts of Value-at-Risk for portfolios of the underlying assets. In practice, comparisons of quantile forecasts of portfolio returns, as generated from multivariate models, often only consider the equal weighted portfolio or some other fixed combination of portfolio constituents, see e.g. McAleer and Da Veiga (2008); Santos et al. (2012); Kole et al. (2017). Considering only a single weight vector can fail to reveal the sensitivity, or the robustness, of the ranking of two models to the choice of weight vector.

A final, very recent, example is the comparison of forecasts using "elementary scoring rules," see Ehm et al. (2016). These authors show that the family of loss functions (or "scoring rules") that are consistent for a given statistical functional (e.g., the mean, a quantile, an expectile) can

be represented as a convex combination of elementary scoring rules. The plot of the elementary scoring rules is called a "Murphy diagram," and Ehm et al. (2016) note that joint testing of the Murphy diagram is not yet fully developed. Ziegel et al. (2017) recently introduced tests for Murphy diagrams based on controlling the family-wise error rate but such corrections can perform poorly in large-scale multiple testing problems, see Hand (1998, p. 115) and White (2000). Moreover, their tests consider only a finite subset of the testable implications instead of a continuum.

This paper develops new out-of-sample tests for multiple testing problems over a continuum of shape parameters, including the above three examples, which do not rely on bounds such as the Bonferroni correction, and which take into account the time series nature of the data used in most forecasting settings. To the best of our knowledge, such tests have not been considered in the literature to date. We consider tests of equal predictive ability (two-sided tests) and superior predictive ability (one-sided tests). We derive our tests using the supremum or average of Diebold-Mariano test statistics for each value of the shape parameter in its range, and obtain critical values using the moving blocks bootstrap of Bühlmann (1995), which is applicable to weakly dependent empirical processes indexed by classes of functions, and is general enough to cover our cases of interest: utility functions and loss functions parameterized by some vector that can take values in a bounded subset of Euclidian space.

Our tests build on the out-of-sample testing framework of Diebold and Mariano (1995) and West (1996). Similar to Giacomini and White (2006) we consider evaluating the forecasting *method*, which, in addition to the forecasting model, includes the estimation scheme and choices of in-sample and out-of-sample periods. White (2000) and Hansen (2005) develop tests of superior predictive ability, using a single loss function, for some model against finitely many alternative models. Our tests differ from the latter tests in that we allow for the joint testing over a continuum of shape parameters rather than a finite subset.

We show via an extensive simulation study that the proposed testing methods have good size and power properties in realistic sample sizes. These positive results stand in stark contrast to the two existing methods used to compare forecasts across a range of loss function parameter values: we find that the Wald test has finite-sample size as high as 50% for a 5% level test, while tests based on a Bonferroni correction suffer, as is often found, from low power.

We consider three empirical applications of the proposed new tests. Firstly, in a comparison of expected utility of equal weighted and minimum-variance portfolio strategies (see DeMiguel

et al. (2007) for an elaboration) we show that our tests are able to reject the null of equal average utility when existing alternative methods cannot. Secondly, we consider a tests of portfolio quantile forecasts generated by multivariate GARCH-DCC and RiskMetrics models, where the portfolio weight vectors live in the unit simplex, and we find that our tests again are able to detect violations of the null hypothesis where existing methods cannot. Finally, we consider tests based on the Murphy diagrams for quantile forecasts generated by GARCH and RiskMetrics models, an application where existing methods simply cannot be applied due to the nature of the testing problem.

The remainder of the paper is structured as follows. In Section 2 we discuss our three illustrative examples. In Section 3 we present the general testing framework and develop our tests. In Section 4 we use Monte-Carlo experiments to study the small sample properties of our tests in settings close to our illustrative examples. In Section 5 we explore these settings empirically. Section 6 concludes.

2 Loss function shape parameters in practice

We consider the following examples of forecast comparison scenarios that we study in Monte-Carlo simulations and empirical illustrations. In all of these examples we will consider loss differences, L, defined as

$$L_{t+1}(\gamma) = S(Y_{t+1}, g_t^{(1)}(\gamma); \gamma) - S(Y_{t+1}, g_t^{(2)}(\gamma); \gamma) \tag{1}$$

where S is the loss function (or scoring rule) for this application, with shape parameter γ taking values in $\Gamma \subset \mathbb{R}^d$, and $g_t^{(i)}(\gamma)$ is the forecast of Y_{t+1} made using model i, which may depend on the shape parameter γ. A test of uniform equal predictive accuracy across all values of the shape parameter examimes:

$$H_0 : E\left[L_{t+1}(\gamma)\right] = 0 \ \forall \ \gamma \in \Gamma \tag{2}$$

$$\text{vs. } H_1 : E\left[L_{t+1}(\gamma)\right] \neq 0 \text{ for some } \gamma \in \Gamma \tag{3}$$

We will also consider tests of uniform superior predictive ability, which consider the hypotheses:

$$H_0' : E\left[L_{t+1}(\gamma)\right] \leq 0 \ \forall \ \gamma \in \Gamma \tag{4}$$

$$\text{vs. } H_1' : E\left[L_{t+1}(\gamma)\right] > 0 \text{ for some } \gamma \in \Gamma \tag{5}$$

2.1 Comparisons based on expected utility

Two forecasting models each generate forecasts of optimal portfolio weights and we seek to compare them in terms of out-of-sample average utility from the resulting portfolio returns. The portfolio returns are obtained as $Y_{t+1}' g_t^{(i)}(\gamma)$, where Y_{t+1} is a vector of returns on the underlying assets, and $g_t^{(i)}(\gamma)$ is the forecasted optimal portfolio weights from model i assuming a preference parameter γ, and per-period utility is computed using some utility function $u(\cdot;\gamma)$. For instance, when $u(\cdot;\gamma)$ is the exponential utility function γ denotes the (scalar) risk aversion parameter, and $\Gamma = [a, b]$, for some $0 < a < b < \infty$. In this case we set

$$S(Y_{t+1}, g_t^{(i)}(\gamma);\gamma) = -u(Y_{t+1}' g_t^{(i)}(\gamma);\gamma) \tag{6}$$

so that lower values of the scoring rule indicate better performance.

2.2 Multivariate forecast comparison based on portfolio characteristics

Let Y_{t+1} denote some vector of returns, and generate portfolio returns as $\tilde{Y}_{t+1}(\gamma) = \gamma' Y_{t+1}$ for some weight vector γ. We are interested in forecasting some statistic ψ_t of $\tilde{Y}_{t+1}(\gamma)$ for all portfolios implied by $\gamma \in \Gamma$. When we consider all long-only portfolios with weights summing to one Γ is the unit simplex. If we consider α-quantile forecasts of the portfolio return, then we may use the "tick" loss function to measure forecast performance and so set

$$S(Y_{t+1}, g_t^{(i)}(\gamma,\alpha);\gamma,\alpha) = (\mathbf{1}\{\gamma' Y_{t+1} \leq g_t^{(i)}(\gamma,\alpha)\} - \alpha)(g_t^{(i)}(\gamma,\alpha) - \gamma' Y_{t+1}). \tag{7}$$

where $\mathbf{1}\{\mathcal{A}\}$ equals one if $\mathcal{A}$ is true and zero otherwise.

2.3 Forecast comparisons via Murphy diagrams

Let Y_{t+1} denote some scalar return, and let ξ_t denote some statistic of Y_{t+1}, such as a mean or quantile. If ξ_t is elicitable, see Gneiting (2011a), then there exists a family of scoring rules (loss

functions), $\mathcal{S}$ such that for any scoring rule $S^* \in \mathcal{S}$ it holds

$$E[S^*(Y_{t+1}, \xi_t)] \leq E[S^*(Y_{t+1}, x)], \ \forall x \in \mathcal{X} \tag{8}$$

where $\mathcal{X}$ is the support of ξ_t. The scoring rule S^* is then said to be "consistent" for the statistic ξ_t. Many statistics, such as the mean, quantile, and expectile, admit families of consistent scoring functions, see Gneiting (2011a). For example, the mean is well-known to be elicitable using the quadratic loss function, and more generally it is elicitable using any "Bregman" loss function. The α-quantile is elicitable using the "tick" loss function, and more generally using any "generalized piecewise linear" (GPL) loss function, see Gneiting (2011b).

In a recent paper, Ehm et al. (2016) show that any scoring rule that is consistent for an expectile (nesting the mean as a special case) or quantile can be represented as a mixture:

$$S^*(Y_{t+1}, x) = \int_{-\infty}^{\infty} \tilde{S}(Y_{t+1}, x; \gamma) dH(\gamma) \tag{9}$$

for some non-negative measure H, and $\gamma \in \Gamma \subset \mathbb{R}$, where $\tilde{S}$ is an "elementary" scoring rule. A plot of the (average) elementary scores across all values of γ is called a "Murphy diagram" by Ehm et al. (2016). If one forecast's Murphy diagram lies below that of another forecast, then the former has lower average loss than the latter for *any* consistent scoring rule.

Comparisons of two forecasts $g_t^{(1)}$ and $g_t^{(2)}$ are usually done using a *single* consistent scoring function (e.g., using mean squared error to compare estimates of the mean), however Patton (2019) shows that the ranking of two forecasts can be sensitive to the choice of specific scoring rule. With the above representation of a consistent scoring rule as a mixture of elementary scoring rules, we can instead consider rankings across *all* consistent scoring rules. For example, to compare α-quantile forecasts we set

$$S(Y_{t+1}, g_t^{(i)}(\alpha); \gamma, \alpha) = (\mathbf{1}\{Y_{t+1} < g_t^{(i)}\} - \alpha)(\mathbf{1}\{\gamma < g_t^{(i)}(\alpha)\} - \mathbf{1}\{\gamma < Y_{t+1}\}) \tag{10}$$

and then test for forecast equality/superiority across all $\gamma \in \mathbb{R}$. The right-hand side of the above equation is the quantile elementary scoring rule from Ehm et al. (2016).

3 Forecast comparison tests in the presence of a loss function shape parameter

Consider the stochastic process $W = \{W_t : \Omega \to \mathbb{R}^{N+s},\ N \in \mathbb{N}_+, s \in \mathbb{N}, t = 1, 2, \ldots\}$ defined on a complete probability space $(\Omega, \mathcal{F}, P)$. We partition the observed vector W_t as $W_t = (Y_t, X_t)$, where $Y_t : \Omega \to \mathbb{R}^N$ is a vector a variables of interest and $X_t : \Omega \to \mathbb{R}^s$ is a vector of explanatory variables. We define $\mathcal{F}_t = \sigma(W_1, \ldots, W_t)$.

To fix notation, we let $|A| = (\mathrm{tr}(A'A))^{1/2}$ denote the Euclidean norm of a matrix A, and $\|A\|_q = (E|A|^q)^{1/q}$ denote the $\mathcal{L}_q$ norm of a random matrix. Finally, $\Rightarrow$ denotes weak convergence with respect to the uniform metric.

We denote the total sample size by T and the out-of-sample size by n. We consider moving or fixed window forecasts generated with in-sample periods of size m, such that the forecast for period $t+1$ is obtained using observations at periods $t-m+1, \ldots, t$ with the moving scheme, and $1, \ldots, m$ with the fixed scheme, respectively.

We consider some (scalar) measurable loss (difference)

$$L_{t+1}(\gamma) = L(W_{t+1}, W_t, \ldots, W_{t-m+1}; \gamma) \tag{11}$$

that takes as arguments $m+1 < \infty$ elements of W and some parameter vector $\gamma \in \Gamma \subset \mathbb{R}^d$ that is independent of W, with Γ a bounded set. As in Giacomini and White (2006), setting $m < \infty$ imposes a limited memory condition on the forecasting methods, which precludes methods with model parameters estimated over expanding windows, but allows for those estimated over fixed and moving windows of finite length.

Below we describe the two-sided tests of equal predictive accuracy, and the one-sided tests of superior predictive accuracy.

3.1 Equal predictive ability tests

Here we consider tests of the following null and alternative hypotheses:

$$H_0 : E\left[L_t(\gamma)\right] = 0 \ \forall\ \gamma \in \Gamma \tag{12}$$

$$\text{vs. } H_1 : \left|E\left[L_t(\gamma^\dagger)\right]\right| \geq \Delta > 0 \text{ for some } \gamma^\dagger \in \Gamma \tag{13}$$

To develop a test of H_0 we use as ingredients the following Diebold-Mariano test statistics (Diebold and Mariano, 1995) as a function of $\gamma \in \Gamma$:

$$t_n(\gamma) \equiv \sqrt{n}\frac{\bar{L}_n(\gamma)}{\hat{\sigma}_n(\gamma)}, \tag{14}$$

with $\bar{L}_n(\gamma) \equiv \frac{1}{n}\sum_{t=m}^{T-1} L_{t+1}(\gamma)$, and $\hat{\sigma}_n^2(\gamma)$ denoting a (strongly) consistent estimator of $\sigma^2(\gamma) \equiv E[L_{t+1}(\gamma)^2]$.

It should be noted that when autocorrelation is present in $L_{t+1}(\gamma)$, $t_n(\gamma)$ does not converge in distribution to a standard normal limit, because $\hat{\sigma}_n^2(\gamma)$ is not a heteroskedasticity and autocorrelation corrected (HAC) estimator of the asymptotic covariance matrix of $\sqrt{n}\bar{L}_n(\gamma)$, see, e.g. Newey and West (1987)). We are not aware of strong uniform law of large numbers results for HAC estimators, which are required in our theoretical results below. As noted by Hansen (2005, under Cor. 3), $\hat{\sigma}_n^2(\gamma)$ does not have to be a consistent estimator of the variance of $\sqrt{n}\bar{L}_n(\gamma)$, because the bootstrap accounts for time series features in the data to obtain critical values of our tests. In some scenarios it might be better not to studentize, and fix $\hat{\sigma}_n^2(\gamma) = 1$ instead. Such scenarios include those for which $\hat{\sigma}_n^2(\gamma)$ is close to zero in small samples.

To test H_0 we employ the test statistics

$$\sup t_n^2 \equiv \sup_{\gamma\in\Gamma} t_n^2(\gamma) \tag{15}$$

$$\text{ave}\, t_n^2 \equiv \int_\Gamma t_n^2(\gamma) dJ(\gamma) \tag{16}$$

where J is some weight function on Γ. In the simplest case, we can set J to be uniform on Γ. Each of the above test statistics can be written as functions $v(t_n)$, where v maps functionals on Γ to $\mathbb{R}$ and we write $t_n = \{t_n(\gamma) : \gamma \in \Gamma\}$ as a random function on Γ. Each function v is continuous with respect to the uniform metric, monotonic in the sense that if $Z_1(\gamma) \leq Z_2(\gamma)$ for all γ then $v(Z_1) \leq v(Z_2)$, and has the property that if $Z(\gamma) \to \infty$ for γ for some subset of Γ with positive mass under weight function J, then $v(Z) \to \infty$.

Under the following assumptions we derive the asymptotic distribution of the test statistics.

Assumption 1. *$\{W_t\}$ is stationary and β-mixing (absolutely regular), with $\beta(t) = c_\beta a^t$, for some finite constant c_β, and $0 < a < 1$.*

Assumption 2. *$E[\sup_{\gamma\in\Gamma} |L_{t+1}|^{4r}] < \infty$, for some $r > 1$, and for all t.*

Assumption 3. $\|L_{t+1}(\gamma) - L_{t+1}(\gamma')\|_{4r} \leq B|\gamma - \gamma'|^{\lambda}$, *for some* $B < \infty$, $\lambda > 0$, *and for all* $\gamma, \gamma' \in \Gamma$, *and* t.

Assumption 4. $\hat{\sigma}_n^2(\gamma) \xrightarrow{a.s.} \sigma^2(\gamma)$ *uniformly over* $\gamma \in \Gamma$. *Moreover,* $\inf_{\gamma \in \Gamma} \sigma^2(\gamma) > 0$.

The β-mixing condition in Assumption 1, which is stronger than α-mixing, but weaker than ϕ-mixing, is usually assumed when deriving functional CLTs for time series data with unbounded absolute moments. Bühlmann (1995) notes that the mixing rate is satisfied for ARMA(p, q) processes with innovations dominated by the Lebesgue measure. Boussama et al. (2011) provides conditions under which multivariate GARCH models satisfy geometric ergodicity, and Bradley et al. (2005, Thm. 3.7) shows that geometric ergodicity implies β-mixing with at least exponential rate, satisfying Assumption 1. Assumption 2 is a standard moment condition, and Assumption 3 requires a Lipschitz condition to hold for these moments. Assumption 4 requires that $\hat{\sigma}_n^2(\cdot)$ satisfies a strong Uniform Law of Large Numbers (see, e.g., Andrews (1992)), and also imposes uniform non-singularity of $\sigma^2(\cdot)$.

Theorem 1. *Let Assumptions 1 to 4 be satisfied. It follows that, for* $m < \infty$, *under* H_0, $\sqrt{n}\bar{L}_n(\cdot) \Rightarrow Z(\cdot)$, *for some Gaussian process* $Z(\cdot)$ *with covariance kernel* $\Sigma(\cdot,\cdot) \equiv \lim_{n\to\infty} Cov\big(\sqrt{n}\bar{L}_n(\cdot), \sqrt{n}\bar{L}_n(\cdot)\big)$. *Moreover, it follows that* $v(t_n) \xrightarrow{d} v(\tilde{t})$, *with* $\tilde{t}(\cdot) \equiv Z(\cdot)/\sigma(\cdot)$.

The following result establishes inference under the null and alternative hypotheses given in equations (12) and (13) above.

Theorem 2. *Let Assumptions 1 to 4 be satisfied, and let* $\Sigma(\cdot,\cdot)$ *be nondegenerate. Under* H_0 *it follows that* $P\left(v(t_n) > c(1-\alpha)\right) \to \alpha = P\left(v(\tilde{t}) > c(1-\alpha)\right)$, *where* $c(1-\alpha)$ *is chosen such that* $P\left(v(\tilde{t}) > c(1-\alpha)\right) = \alpha$. *Moreover, let* $\Gamma^{\dagger} = \{\gamma : |\gamma - \gamma^{\dagger}|^{\lambda} < \Delta/B\}$ *have positive* J*-measure. Under* H_1 *it follows that* $v(t_n) \xrightarrow{d} \infty$, *and* $P\big(v(t_n) > c(1-\alpha)\big) \to 1$.

We establish the consistency of the block bootstrap for general empirical processes of Bühlmann (1995) for $v(t_n)$. The block bootstrap was first studied by Künsch (1989) for general stationary observations.

The bootstrap counterpart of $\sqrt{n}\bar{L}_n(\gamma)$ is given by

$$\sqrt{n}\bar{L}_n^*(\gamma) \equiv \sqrt{n}\frac{1}{n}\sum_{t=m}^{T-1}\big(L_{t+1}^*(\gamma) - \mu_n^*(\gamma)\big), \tag{17}$$

with $\mu_n^*(\gamma) \equiv \frac{1}{n-l+1}\sum_{i=1}^{n-l+1}\frac{1}{l}\sum_{t=m+i}^{m+i+l-1} L_t(\gamma)$ denoting the expectation of $\frac{1}{n}\sum_{t=m}^{T-1} L_{t+1}^*(\gamma)$ conditional on the original sample, l denoting the block length, and $L_{t+1}^*(\gamma)$ denoting the bootstrap

counterpart of $L_{t+1}(\gamma)$. Similarly, let $t_n^*(\gamma) \equiv \sqrt{n}\bar{L}_n^*(\gamma)/\hat{\sigma}_n(\gamma)$, and let $c_n^*(1-\alpha)$ denote the α-quantile of $t_n^*(\gamma)$.

We impose the following condition on the rate that $l = l(n) \to \infty$, as $n \to \infty$.

Assumption 5. *The block length l satisfies $l(n) = O(n^{1/2-\varepsilon})$, for some $0 < \varepsilon < 1/2$.*

The following result establishes consistency of the bootstrap.

Theorem 3. *Let the assumptions of Theorem 1 and Assumption 5 hold. Under H_0 it follows that $\sqrt{n}\bar{L}_n^*(\cdot) \Rightarrow Z(\cdot)$ almost surely. Moreover, $P(v(t_n) > c_n^*(1-\alpha)) \to \alpha$.*

Theorem 3 shows that we can estimate $c_n^*(1-\alpha)$ through simulation: let $c_n^B(1-\alpha)$ denote the $\alpha \cdot 100\%$ percentile of the test statistics $v(t_n^{*(1)}(\gamma)), \ldots, v(t_n^{*(B)}(\gamma))$ obtained from B bootstrap samples. As $B \to \infty$, $c_n^B(1-\alpha)$ becomes arbitrarily close to $c_n^*(1-\alpha)$.

3.2 Superior predictive ability tests

The results of the previous section allow us to easily also consider tests of uniform superior predictive ability, which consider the hypotheses:

$$H_0' : E\left[L_{t+1}(\gamma)\right] \leq 0 \ \forall \ \gamma \in \Gamma \tag{18}$$

$$\text{vs. } H_1' : E\left[L_{t+1}(\gamma^\dagger)\right] \geq \Delta > 0 \text{ for some } \gamma^\dagger \in \Gamma \tag{19}$$

Notice that H_0 in Equation (12) is the element of H_0' least favorable to the alternative. We can thus construct a valid test of H_0' from

$$\sup t_n \equiv \sup_{\gamma \in \Gamma} t_n(\gamma). \tag{20}$$

The results under H_0 in Theorems 1, 2, and 3 hold for H_0' for a demeaned version of $\sup t_n$, defined as

$$\sup \tau_n \equiv \sqrt{n}\frac{\bar{L}_n(\gamma) - E[\bar{L}_n(\gamma)]}{\hat{\sigma}_n(\gamma)}. \tag{21}$$

We must use $\sup \tau_n$ because H_0' allows for $E[\bar{L}_n(\gamma)] < 0$. Note that we can obtain valid critical values under H_0' from Theorem 3. Further, the result in Theorem 2 under H_1 also holds under H_1' for $\sup t_n$ (not just for $\sup \tau_n$), which implies that $\sup t_n$ has asymptotic power against fixed alternatives in this setting as well.

3.3 Practical implementation

When $\Gamma \in \mathbb{R}^d$ contains infinitely many elements we cannot evaluate the test statistics over all elements of Γ in practice. Here we provide two numerical approximations to our test statistics for which Theorems 1 and 2 remain valid.

We first look at discretizations of Γ that become increasingly dense. Consider a grid of Γ with K_n elements Γ_n^i, such that $\sup_{\gamma,\gamma' \in \Gamma_n^i} |\gamma - \gamma| < \delta_n$, for all $i = 1, \ldots, K_n$, and let $\gamma_{n,i}$ be some point in Γ_n^i. We have the following approximations to our test statistics:

$$\widehat{\operatorname{ave} t_n^2} \equiv \sum_{i=1}^{K_n} t_n^2(\gamma_{n,i}) \int_{\Gamma_n^i} dJ(\gamma), \tag{22}$$

$$\widehat{\sup t_n^2} \equiv \max_{i=1,\ldots,K_n} t_n^2(\gamma_{n,i}), \text{and} \tag{23}$$

$$\widehat{\sup t_n} \equiv \max_{i=1,\ldots,K_n} t_n(\gamma_{n,i}). \tag{24}$$

If Γ is a hyperrectangle in $\mathbb{R}^d$, a particularly convenient choice of J, K_n, and $\{\Gamma_n^i\}_{i=1}^{K_n}$ derives from partitioning each dimension of Γ in v_n equal parts, which results in $K_n = v_n^d$. Choosing J to be uniform over Γ gives $\int_{\Gamma_n^i} dJ(\gamma) = v_n^{-d}$, which is simple to implement. Other choices of J may require more involved algebra or simulations to obtain $\int_{\Gamma_n^i} dJ(\gamma)$.

The condition that $\delta_n \to 0$ implies that K_n grows quickly with large d. As a result the calculation of $\widehat{\operatorname{ave} t_n^2}$, $\widehat{\sup t_n^2}$, and $\widehat{\sup t_n}$ becomes problematic for large n. In such cases one can instead use Monte Carlo simulations from J to obtain approximations of the test statistics. Consider S_n independent draws $\gamma^{(i)}$ from J, $i = 1, \ldots, S_n$, and the approximations:

$$\widetilde{\operatorname{ave} t_n^2} \equiv \frac{1}{S_n} \sum_{i=1}^{S_n} t_n^2(\gamma^{(i)}), \tag{25}$$

$$\widetilde{\sup t_n^2} \equiv \max_{i=1,\ldots,S_n} t_n^2(\gamma^{(i)}), \text{and} \tag{26}$$

$$\widetilde{\sup t_n} \equiv \max_{i=1,\ldots,S_n} t_n(\gamma^{(i)}). \tag{27}$$

Proposition 1. *Let the assumptions of Theorem 1 hold. Moreover, let the weight function J be absolutely continuous. For some $K_n \to \infty$, such that $\delta_n \to 0$, as $n \to \infty$, $\widehat{v(t_n)} \xrightarrow{p} v(t_n)$. Moreover, $\widetilde{v(t_n)} \xrightarrow{p} v(t_n)$ for $S_n \to \infty$ as $n \to \infty$.*

3.4 Benchmark testing methods

For comparison with the proposed new tests, we consider standard joint Wald tests and the Bonferroni multiple-comparison correction as benchmarks to the tests proposed above. It should be noted that these tests can only be applied at a finite number of points, M, in Γ, and therefore cannot generally test over all Γ.

Consider some discrete parameter set $\Gamma_M = \{\gamma_1, \ldots, \gamma_M\} \subset \Gamma$. We define the standard Wald test statistic as

$$\hat{Q}_n^h \equiv n\tilde{L}_n(\Gamma_M)'\hat{\Omega}_{M,n}^{-1}\tilde{L}_n(\Gamma_M), \tag{28}$$

where $\tilde{L}_n(\Gamma_M) \equiv \left(\bar{L}_n(\gamma_1)', \ldots, \bar{L}_n(\gamma_M)'\right)'$, and $\hat{\Omega}_{M,n}$ is some HAC estimator of the asymptotic covariance matrix of $\sqrt{n}\tilde{L}_n(\Gamma_M)$, e.g., the estimator of Newey and West (1987).

A two-sided α-level test rejects the null hypothesis when $\hat{Q}_n^h > \chi^2_{M,1-\alpha}$, where $\chi^2_{M,1-\alpha}$ denotes the $(1-\alpha)$-quantile of a χ^2 distribution with M degrees of freedom. As M increases $\hat{\Omega}_{M,n}$ becomes near-singular, which can lead to erratic behavior in the test statistic (and we observe such behavior in our simulation study below).

A two-sided α-level test using the Bonferroni correction rejects the null hypothesis if, for at least one $\gamma \in \Gamma_M$, we find $n\bar{L}_n^2(\gamma)/\tilde{\sigma}_n^2(\gamma) > \chi^2_{1,1-\alpha/M}$, with $\tilde{\sigma}_n^2(\gamma)$ a HAC asymptotic covariance estimator of $\sqrt{n}\bar{L}_n(\gamma)$. Tests using the Bonferroni correction are conservative for large M, and also whenever the test statistics are positively correlated.

A one-sided α-level test using the Bonferroni correction rejects the null hypothesis if, for at least one $\gamma \in \Gamma_M$, we find $n\bar{L}_n(\gamma)/\tilde{\sigma}_n(\gamma) > z^{-1}_{1-\alpha/M}$, with $z^{-1}_{1-\alpha}$ denoting the $(1-\alpha)$-quantile of the standard normal distribution. We do not consider one-sided Wald tests as a benchmark here, although they may be constructed using, e.g., the methods of Wolak (1987, 1989).

4 Simulation studies

In this section we evaluate the finite-sample performance of our proposed tests in the three applications described in Section 2. In Sections 4.1–4.3 below we describe the simulation designs for each of these applications, and in Section 4.4 we present the results.

4.1 Comparisons based on expected utility

We consider the difference in expected utility of two commonly used portfolio management strategies: the equal weighted portfolio and the minimum-variance portfolio. See DeMiguel et al. (2007) for an in-depth analysis of these, and other, portfolio strategies. For a $N \times 1$ vector of monthly excess returns Y_{t+1} these strategies can be defined in terms of portfolio weight vectors:

$$\begin{aligned} w_{t+1}^{\text{eq}} &= \frac{1}{N}\iota, \\ w_{t+1}^{\text{mv}} &= \frac{1}{\iota'\Sigma_{t+1}^{-1}\iota}\Sigma_{t+1}^{-1}\iota, \end{aligned} \tag{29}$$

with $\Sigma_{t+1} = \text{Cov}(Y_{t+1})$, and ι a $N \times 1$ vector of ones. Denote the portfolio returns as $Y_{t+1}^{\text{eq}} = w_{t+1}^{\text{eq}\prime} Y_{t+1}$, and $Y_{t+1}^{\text{mv}} = w_{t+1}^{\text{mv}\prime} Y_{t+1}$. The feasible counterpart of w_{t+1}^{mv} depends on an estimate of Σ_{t+1}. We consider a rolling window estimate of the covariance matrix based on the most recent 120 observations, corresponding to 10 years of monthly returns data.

We test whether the equal weighted and minimum-variance portfolio returns have equivalent expected utility across a range of levels of risk aversion. We model utility with the exponential utility function $u(y;\gamma) = -e^{-\gamma y}/\gamma$. A wide range of values of the risk aversion parameter γ have been reported in the literature, ranging from near zero to as high as 60, see Bliss and Panigirtzoglou (2004). These authors estimate this parameter as being between 2.98 to 10.56, while DeMiguel et al. (2007) perform a batch of comparisons for investors with risk aversion ranging between 1 and 10. Based on this, we test for equal expected utility over $\Gamma = [1, 10]$. We draw uniformly over this range when implementing the ave-test.

We generate the excess returns Y_{t+1} according to a one-factor model, based on the DGP in the simulation study of DeMiguel et al. (2007). Let $Y_{t+1} = (Y_{t+1}^f, Y_{1,t+1}, \ldots, Y_{N-1,t+1})'$, with Y_{t+1}^f denoting the excess return on the factor portfolio, and the $Y_{i,t+1}$ denoting the $N-1$ excess returns generated as

$$\begin{aligned} Y_{i,t+1} &= \alpha_i + \beta_i Y_{t+1}^f + \eta_{i,t+1}, \\ \nu_{i,t+1} &\sim \text{iid}\,\mathcal{N}(0, \sigma_{\eta,i}^2), \\ Y_{t+1}^f &\sim \text{iid}\,\mathcal{N}(\mu_f, \sigma_f^2). \end{aligned} \tag{30}$$

We follow the parameterization of DeMiguel et al. (2007), which resembles estimates that

are commonly found in empirical studies. We set $\alpha_i = 0$, and $\beta_i = 0.5 + (i-1)/(N-1)$, for all $i = 1, \ldots, N-1$. Moreover, we set $\mu_f = 8\%$, and $\sigma_f = 16\%$. Finally, we let the idiosyncratic volatilities vary between 10% and 30%. However, unlike DeMiguel et al. (2007), who draw from the uniform distribution on $[10\%, 30\%]$, we opt for deterministic cross-sectional variation between 10% and 30% by setting $\sigma_{\eta,i} = 10\% + 20\% \cdot \sin(\pi(i-1)/(N-1))$. We do so to facilitate the approximation of $E[L_{t+1}(\gamma)]$, which is required in the size experiment.

Given the portfolio strategies we consider, it is not generally possible to find a parameterization that implies $E[L_{t+1}(\gamma)] = 0$ for all $\gamma \in \Gamma$. In the size experiment we therefore test the null hypotheses at $E[L_{t+1}(\gamma)] = \zeta_m(\gamma)$ instead of zero, where $\zeta_m(\gamma)$ is the population value of $E[L_{t+1}(\gamma)]$, which we estimate using 100,000 simulations.

4.2 Forecast comparison via tail quantile forecasts of portfolio returns

We next study a scenario comparing quantile forecasts of portfolio returns implied by multivariate forecasting models. We model the financial assets using a GARCH-DCC model (Engle, 2002) with normal errors, parameterized to resemble the properties of daily asset returns.

We compare two widely-used models: (i) a fully parameterized GARCH-DCC model with normal errors, and (ii) a multivariate normal distribution with the RiskMetrics covariance estimator (Riskmetrics, 1996). We let the $N \times 1$ return vector Y_{t+1} follow a GARCH-DCC process

$$
\begin{aligned}
Y_{t+1} &= \mu_t + H_{t+1}^{1/2} C_{t+1}^{1/2} \nu_{t+1}, \\
\nu_{t+1} &= (\nu_{t+1,1}, \ldots, \nu_{t+1,N})' \sim iid\, N(0, I), \\
H_{t+1} &= \operatorname{diag}(h_{t+1,1}, \ldots, h_{t+1,N}), \\
h_{t+1,i} &= \omega_0 + \omega_1 h_{t,i} + \omega_2 h_{t,i} \nu_{t,i}^2, \\
C_{t+1} &= \operatorname{diag}\left(\tilde{C}_{t+1}\right)^{-1/2} \tilde{C}_{t+1} \operatorname{diag}\left(\tilde{C}_{t+1}\right)^{-1/2}, \\
\tilde{C}_{t+1} &= (1 - \xi_1 - \xi_2)\bar{C} + \xi_1 \tilde{C}_t + \xi_2 \nu_t \nu_t', \\
\bar{C} &= [\bar{C}]_{ij}, \text{ where } [\bar{C}]_{ij} = 1 - \frac{|i-j|}{N}.
\end{aligned}
\tag{31}
$$

We choose GARCH parameters $\omega_0 = 0.05$, $\omega_1 = 0.10$, $\omega_2 = 0.85$ and DCC parameters $\xi_1 = 0.025$, $\xi_2 = 0.95$, to match time-varying volatility and correlation patterns commonly found in daily equity returns. We set $\mu_t = 0$ for simplicity. To fix the value of $\bar{C}$ we use the covariance matrix generated by a Bartlett kernel with bandwith set to N. This specification generates a diverse set of correlations, and ensures positive definiteness of $\bar{C}$.

We are interested in one-period-ahead α-quantile forecasts for portfolio returns $\tilde{Y}_{t+1}(\gamma) = \gamma' Y_{t+1}$, with $\alpha = 5\%$, for all $\gamma \in \Gamma$. The first forecast we consider is the optimal forecast based on the GARCH-DCC model above. This forecast is given by

$$Q^{(1)}_{t+1,\alpha}(\gamma) = \Phi^{-1}(\alpha) \cdot \gamma' H_t^{1/2} C_t H_t^{1/2} \gamma, \tag{32}$$

where $\Phi^{-1}(\alpha)$ denotes the α-quantile of the standard normal distribution.

The RiskMetrics forecast is

$$Q^{(2)}_{t+1,\alpha}(\gamma) = \Phi^{-1}(\alpha) \cdot \gamma' \hat{\Sigma}_{t+1} \gamma, \tag{33}$$

$$\text{where } \hat{\Sigma}_{t+1} = c_l(1-\lambda) \sum_{j=0}^{m} \lambda^j \left(Y_{t-j+1} - \hat{\mu}_t\right)\left(Y_{t-j+1} - \hat{\mu}_t\right)' \tag{34}$$

with $\hat{\mu}_t = \frac{1}{m}\sum_{j=1}^{m} Y_{t-j+1}$, and c_l a constant that normalizes the summed weights $(1-\lambda)\sum_{j=0}^{m}\lambda^j$ to one. As is standard for the RiskMetrics approach using daily returns, we set $\lambda = 0.94$.

We obtain the scores (losses) $S^{(i)}_{t+1}(\gamma)$ using the tick-loss function, which is a consistent loss function for the quantile, and is defined as

$$S^{(i)}_{t+1}(\gamma, \alpha) = \left(\mathbb{1}\left\{\tilde{Y}^p_{t+1}(\gamma) < Q^{(i)}_{t+1,\alpha}(\gamma)\right\} - \alpha\right)\left(Q^{(i)}_{t+1,\alpha}(\gamma) - \tilde{Y}^p_{t+1}(\gamma)\right), \tag{35}$$

and obtain loss differences $L_{t+1}(\gamma) = S^{(2)}_{t+1}(\gamma) - S^{(1)}_{t+1}(\gamma)$.

We consider all portfolio return vectors with positive weights summing to one, i.e. $\Gamma = \{\gamma : \gamma_i \geq 0, i = 1, \ldots, N, \sum_{i=1}^{N}\gamma_i = 1\}$. Γ is also known as the $(N-1)$-simplex, and drawing uniformly from Γ is particularly easy using the Dirichlet distribution of order N with concentration parameters set to one. See Kotz et al. (2000, Ch. 49) for an elaborate treatment of the Dirichlet distribution.

As in the previous example, to study the finite-sample size of this test we consider the null hypothesis that $E[\bar{L}_n(\gamma)] = \zeta_m(\gamma)$ instead of zero, where $\zeta_m(\gamma)$ is the population value of $E[L_{t+1}(\gamma)]$, which we estimate using 100,000 simulations.

4.3 Forecast comparison via Murphy diagrams of quantile forecasts

Under mild regularity conditions (see, e.g., Gneiting (2011a)) the (conditional) α-quantile of a random variable Y_{t+1} is elicitable using the "generalized piecewise linear" (GPL) class of scoring

rules:

$$S(Y_{t+1}, x; \alpha, g) = \big(\mathbb{1}(Y_{t+1} < x) - \alpha\big)\big(g(Y_{t+1}) - g(x)\big), \tag{36}$$

where $g(\cdot)$ is a non-decreasing function. A commonly used member of this family is the tick-loss function, which sets $g(z) = z$, and which was used in the previous section. In this example we test for differences in predictive ability of competing α-quantile forecasts across the set of all consistent scoring rules for α-quantiles, denoted $\mathcal{S}^{\alpha}_{GPL}$, using the mixture representation for this class of loss functions presented in Ehm et al. (2016):

$$S(Y_{t+1}, x; \alpha, g) = \int_{-\infty}^{\infty} \tilde{S}(Y_{t+1}, x; \alpha, \gamma) dH(\gamma; g) \tag{37}$$

$$\text{where } \tilde{S}(Y_{t+1}, x; \alpha, \gamma) = \big(\mathbb{1}(Y_{t+1} < x) - \alpha\big)\big(\mathbb{1}(\gamma < x) - \mathbb{1}(\gamma < Y_{t+1})\big), \tag{38}$$

where $H(\cdot; g)$ some non-negative measure.

Consider two forecasts $Q^{(1)}_{t+1,\alpha}$ and $Q^{(2)}_{t+1,\alpha}$. We say that $Q^{(2)}_{t+1,\alpha}$ dominates $Q^{(1)}_{t+1,\alpha}$ if

$$\begin{aligned} E_t[L(Y_{t+1}, Q^{(1)}_{t+1,\alpha}, Q^{(2)}_{t+1,\alpha}, \alpha, g)] &\equiv E_t[S(Y_{t+1}, Q^{(2)}_{t+1,\alpha}, \alpha, g) - S(Y_{t+1}, Q^{(1)}_{t+1,\alpha}, \alpha, g)] \\ &\leq 0 \text{ for all } S \in \mathcal{S}^{\alpha}_{GPL} \end{aligned} \tag{39}$$

Corollary 1 in Ehm et al. (2016) establishes that $Q^{(2)}_{t+1,\alpha}$ dominating $Q^{(1)}_{t+1,\alpha}$ is implied by

$$\begin{aligned} E_t[\tilde{L}(Y_{t+1}, Q^{(1)}_{t+1,\alpha}, Q^{(2)}_{t+1,\alpha}, \alpha, \gamma)] &\equiv E_t[\tilde{S}(Y_{t+1}, Q^{(2)}_{t+1,\alpha}, \alpha, \gamma) - \tilde{S}(Y_{t+1}, Q^{(1)}_{t+1,\alpha}, \alpha, \gamma)] \\ &\leq 0 \text{ for all } \gamma \in \mathbb{R} \end{aligned} \tag{40}$$

We can therefore test for equal predictive ability by testing the above condition. It should be noted that our theory requires the range of γ, denoted Γ, to be bounded, and so we cannot test over all $\gamma \in \mathbb{R}$. However, in practice we can make Γ large enough to cover all relevant parameter values, since $\tilde{S}(Y_{t+1}, Q^{(2)}_{t+1,\alpha}; \alpha, \gamma) - \tilde{S}(Y_{t+1}, Q^{(1)}_{t+1,\alpha}; \alpha, \gamma)$ is known to be identically zero for $\gamma \notin \big[\min\big(Y_{t+1}, Q^{(1)}_{t+1,\alpha}, Q^{(2)}_{t+1,\alpha}\big), \max\big(Y_{t+1}, Q^{(1)}_{t+1,\alpha}, Q^{(2)}_{t+1,\alpha}\big)\big]$.

In small samples it can occur that $\tilde{S}(Y_{t+1}, Q^{(2)}_{t+1,\alpha}; \alpha, \gamma) - \tilde{S}(Y_{t+1}, Q^{(1)}_{t+1,\alpha}; \alpha, \gamma) = 0$ for all observations in a given sample, for some values of γ. As a result, $\hat{\sigma}^2_n(\gamma) = 0$ for these values of γ. To circumvent this we fix $\sigma^2_n(\gamma) = 1$ for all $\gamma \in \Gamma$, i.e. we consider sup- and ave-tests based on $t_n(\gamma) \equiv \sqrt{n}\bar{L}_n(\gamma)$ instead of $t_n(\gamma) \equiv \sqrt{n}\frac{\bar{L}_n(\gamma)}{\hat{\sigma}_n(\gamma)}$. The p-values remain valid under the

bootstrap. The HAC covariance estimators used in the calculation of the multivariate Wald test and the Bonferroni-corrected test suffer from the same singularity. However, inference is no longer valid for these tests, because the limit law of these test statistics is no longer standard without studentization.

We use the same quantile forecast models as in the simulation design in the previous section, but set $N = 1$, so that the quantile forecasts defined in Equations (32) and (33) are obtained from a GARCH model instead of a GARCH-DCC model. For additional comparison, we also consider a rolling window sample quantile estimated over the previous 250 days.

As in the previous examples, to study the finite-sample size of this test we consider the null hypothesis that $E[\bar{L}_n(\gamma)] = \zeta_m(\gamma)$ instead of zero, where $\zeta_m(\gamma)$ is the population value of $E[L_{t+1}(\gamma)]$, which we estimate using 100,000 simulations.

4.4 Simulation results

Table 1 presents rejection rates for the size and power experiments introduced in Section 4.1, based on 1,000 Monte-Carlo simulations. We consider out-of-sample period lengths $n = 120$ and 600 observations, corresponding to 10 and 50 years of monthly returns data. We consider increasingly large grids of Γ, with the number of grid points set to $K_n = 1, 10, 50, 100$, and 250. We obtain critical values using $B = 1{,}000$ bootstrap samples.

From Panel A we observe that the (two-sided) sup-t^2 and ave-t^2 tests are somewhat oversized for $n = 120$ out-of-sample observations, and appropriately sized for $n = 600$. The one-sided sup-t test is also oversized for $n = 120$ but approximately correctly sized for $n = 600$. Reassuringly, we observe that the sup-t^2, ave-t^2 and sup-t tests are stable in terms of rejection rates once K_n is moderately large, indicating robustness to this tuning parameter.

The benchmark tests (based on a Wald test or a Bonferroni correction) perform poorly as K_n increases, with the Wald test having large size distortions, and the Bonferroni-corrected test becoming conservative. This sensitivity can be avoided by implementing these tests on just a single value of γ, though of course in that case the conclusion of the test is sensitive to the particular choice of γ.

Panel B shows rejection rates in the power experiment. We observe the sup- and ave-test rejection probabilities being stable once the value of K_n is moderately large. In contrast, but as anticipated, the Bonferroni-adjusted tests have power declining with K_n. The power of the Wald test in this application also declines with K_n, and we note that this test cannot be implemented

when $n = 120$ and $K_n = 250$ as in that case the covariance matrix is singular.

[Table 1 about here.]

Table 2 presents small sample rejection rates of the size and power experiments introduced in Section 4.2, for portfolios composed of 30 assets. Results are presented for sample sizes of $n = 500$ and 2,000 observations, corresponding approximately to two and eight years of daily asset returns, and six sets of weight vectors, which are drawn as follows. We first consider a set of 31 deterministic weight vectors: the equal weighted portfolio weights and the 30 basis vectors. Subsequently we randomly draw $S_n - 31$ weight vectors from J, for $S_n = 50, 100, 250, 500$ and 1,000. We use $B = 1{,}000$ bootstrap samples to obtain critical values.

Panel A provides rejection rates in the size experiment. We observe that the sup-t^2, ave-t^2 and sup-t tests have reasonable size properties, although the tests are slightly conservative for n =2,000 (rejection rates between 1-2%). The same holds for the Bonferroni-corrected tests at all S_n. The benchmark Wald test is oversized for all S_n at $n = 500$, and for all S_n larger than 31 at $n = 2{,}000$, illustrating the problems with this test as S_n grows. As in the previous example, the rejection rates of the sup-t^2, ave-t^2 and sup-t tests are stable across S_n.

Panel B shows rejection rates in the power experiment. As in the previous section, we observe the sup- and ave-test rejection probabilities being stable across values of S_n. We again observe the Bonferroni-adjusted tests having decreasing power as S_n increases. The power of the Wald test in this application increases, driven by its failure to control size as S_n increases.

[Table 2 about here.]

Table 3 provides small sample rejection rates of the tests in size and power experiments introduced in Section 4.3. The sample sizes considered are $n = 500$ and $n = 2{,}000$, corresponding approximately to two and eight years of daily returns data. We consider grids of Γ with $K_n = 50, 100$, and 250 grid points equally spaced over the interval $[-20, 0]$. We select this interval because outside of it the elementary score differences are equal to zero in almost all realizations. As we cannot always (across values of γ in the elementary scores) compute the asymptotic covariance required to obtain the benchmark Wald and Bonferroni-corrected tests, we do not implement those tests here. Instead, we present the results of a standard Diebold-Mariano test based on the tick-loss function as benchmark. These are reported in the rows labeled "1".

Panels A and B provide rejection rates for the size experiments. In Panel A we compare the GARCH and RiskMetrics forecasts. We observe that the sup-t^2 and ave-t^2 tests are correctly sized at both out-of-sample period lengths considered (n = 500 and 2,000). The one-sided sup-t test is slightly conservative at n = 500, but is close to nominal rates for n = 2,000. The benchmark Diebold-Mariano test using the tick-loss function, is also approximately correctly sized. The rejection rates of the sup- and ave-tests are stable across values K_n, indicating robustness to this tuning parameter. Panel B provides rejection rates for the size experiment where we compare the GARCH and the rolling window quantile forecasts. We find that the two-sided Diebold-Mariano test and the ave-t^2-test are oversized, whereas the sup-t^2 and sup-t tests have reasonable rejection rates.

Panel C provides rejection rates in the power experiment in which we compare the GARCH and RiskMetrics forecasts. We observe that this particular alternative is not very distant from the null, and the ave- and sup-tests have no power at n = 500. At n = 2,000 the proposed tests have power against the alternative, but the benchmark test is more powerful. Panel D provides rejection rates in the power experiment comparing the GARCH and rolling window quantile forecasts. The sup- and ave-tests reject more often, and have power properties similar to the benchmark Diebold-Mariano test.

[Table 3 about here.]

5 Applications to equity return forecast environments

5.1 Comparing the utility of two portfolio strategies

In this section we compare equal weighted and minimum-variance portfolio strategies in terms of average utility, across a range of levels of risk aversion. We use monthly returns data on 30 U.S. industry portfolios, from September 1926 to December 2017, a total of 1,098 observations.[1] The minimum-variance portfolio weights are estimated over a rolling window of m = 120 months. We use the exponential utility function $u(y;\gamma) = -e^{-\gamma y}/\gamma$, with $\gamma \in [1, 10]$, which covers all risk aversion parameter values considered in DeMiguel et al. (2007).

Table 4 provides p-values for the proposed new tests, as well as the benchmark Wald and Bonferroni-adjusted tests. The left panel presents results for tests of the null of equal predictive

[1]The returns can be obtained from the data library at `http://mba.tuck.dartmouth.edu/pages/faculty/ken.french/data_library.html`

ability for these two portfolio strategies, while the right panel presents results for one-sided tests of the null that the minimum-variance portfolio strategy is not worse than the equal weighted strategy. The row labeled $K_n = 1$ tests the hypothesis of equal predictive ability for risk aversion $\gamma = 2.5$, while the remaining rows use $K_n = 10, 50, 100, 250$ equally-spaced points in $[1, 10]$.

When $K_n = 1$, the null of equal predictive ability is rejected using all tests. We also find that the one-sided test rejects the null, indicating that the equal weighted portfolio generates significantly higher out-of-sample utility than the minimum-variance portfolio, for this level of risk aversion. When we increase K_n, and test the hypothesis of equal average utility over the entirety of Γ, we find that the ave-t^2 test fails to reject the null, while the sup-t^2 test continues to reject the null. The one-sided test using the new sup-t test also rejects the null for all values of K_n.

Looking at the benchmark tests, the Bonferroni-corrected test cannot reject the null hypothesis for larger values of K_n. This finding is consistent with the conservativeness of this test as K_n increases documented in the simuation study in the previous section. The Wald test rejects the null hypothesis for all values of K_n except $K_n = 250$, but since the simulation exercise shows the test has severe size distortions, we should not rely on conclusions drawn form the Wald test.

Figure 1 shows the sample mean of expected utility differences and the pointwise 95% confidence bounds for each $\gamma \in [1, 10]$. We observe that for γ less than about 3, the confidence interval does not include zero, indicating that for lower levels of risk aversion the equal weighted portfolio significantly outperforms the minimum-variance portfolio. For higher levels of risk aversion, the pointwise confidence intervals either contain zero, or lie below zero. Since the sup-t^2 test considers the largest deviation from the zero line, while the ave-t^2 considers (weighted) averages of all deviations, it is intuitive that the ave-t^2 test statistic indicates weaker evidence against the null due to the large subinterval of Γ for which the mean utility differential is insignificantly different from zero.

Panels B and C of Table 4 show results for $\Gamma = [1, 5]$ and $\Gamma = [5, 10]$, to examine the sensitivity of the conclusions of these tests to the range of values of risk aversion considered. For less risk averse investors, with $\Gamma = [1, 5]$, we see that the both the ave-t^2 and the sup-t^2 tests reject the null-hypothesis. If we consider more risk averse investors, with $\Gamma = [5, 10]$, we see that the null hypothesis cannot be rejected by either the ave- or the sup-tests. Conclusions drawn from the Bonferroni-corrected tests do not change much, with both tests failing to reject the null hypothesis for larger values of K_n.

[Figure 1 about here.]

[Table 4 about here.]

5.2 Quantile forecasts of portfolio returns from multivariate models

In this analysis we compare two multivariate volatility models, a GARCH-DCC model and the RiskMetrics model, by the quality of their forecasts for the 5% quantile (i.e., the 5% Value-at-Risk) of the returns on portfolios of the underlying assets. We use daily returns on the same 30 U.S. industry portfolios as in the previous section, over the period January 1998 to December 2017, a total of 5,032 observations. The GARCH-DCC model is estimated over a rolling window of 1,000 observations. The one-sided tests take the GARCH-DCC model as the benchmark, and a rejection of the one-sided null provides evidence that the RiskMetrics has lower average loss than the GARCH-DCC model for some portfolios in the unit simplex.

We consider the following sets of portfolios. For $S_n = 1$ we consider only the equal weighted portfolio. For $S_n = 31$ we consider the equal weighted portfolio and all 30 single-asset portfolios. For $S_n > 31$, we randomly draw portfolio weight vectors from the 30-dimensional simplex.

Table 5 presents p-values of the tests of equal or superior predictive ability. We show results for the full sample, as well as the first and second halves of the sample period. The results for the full sample show that the models have approximately equal performance, since the null hypotheses of equal or superior predictive ability cannot be rejected. We note that that the sup- and ave-tests generate p-values that are stable for larger values of S_n, whereas the Bonferroni p-values approach one as S_n increases, consistent with the conservativeness of this test found in the simulation study. The Wald tests are unreliable for larger values S_n, as shown in the simulation exercises, and are not reported for $S_n > 31$.

In Panel B of Table 5 we find evidence against the null of equal predictive accuracy using the sup-t test, with p-values around 0.04 to 0.06. The one-sided test generates p-values of 0.02 to 0.04, indicating evidence that the RiskMetrics model significantly outperforms the GARCH-DCC model for part of the shape parameter space (i.e., for some portfolio weight vectors). In the second sub-sample we cannot reject the hypotheses of equal or superior predictive ability using any test. Again the sup- and ave-tests, have stable p-values for larger S_n, whereas the Bonferroni p-values increase with S_n.

Figure 2 plots the sample mean of the tick-loss differences and the 95% confidence bounds for the first 100 portfolio weights that we draw, over the full sample and subsamples, and sorted on mean tick loss difference. In the first half of the sample we indeed find that the RiskMetrics forecasts perform better, although for only few portfolio vectors we observe (pointwise) confidence intervals that exclude zero. The sup-tests detect the outperformance of the RiskMetrics forecasts better than the ave-test as observed in Table 5. In the second half of the sample the average tick-loss differences are generally negative, which is in agreement with the null of weakly better GARCH-DCC forecasts.

[Figure 2 about here.]

[Table 5 about here.]

5.3 Quantile forecast comparison via Murphy diagrams

Our final empirical analysis compares two forecast models for the 5% quantile (i.e., the 5% Value-at-Risk) of a single asset. We compare three models: a GARCH(1,1) model (Bollerslev, 1986), the RiskMetrics model, and a simple rolling window sample quantile calculated over the previous 250 days. We use the same data as the previous sub-section: daily returns on 30 U.S. industry portfolios, over the period January 1998 to December 2017, a total of 5,032 observations. The GARCH model is estimated over a rolling window of 1,000 observations. The one-sided tests take the GARCH model as the benchmark model. The parameter space for the elemetary scoring rule shape parameter (see Section 4.3 for details) is $\Gamma = [-20, 0]$, and we consider an increasingly fine grid of equally-spaced points in this space when implementing the new tests.

We set the GARCH forecast as benchmark against forecasts from the RiskMetrics and rolling window sample quantile models (i.e. we subtract the loss of the alternative forecasts from the GARCH forecast loss). A rejection of the one-sided null therefore implies that the RiskMetrics or rolling window sample quantile forecasts significantly outperform the GARCH forecast.

We implement the tests for each of the 30 portfolio returns separately. Table 6 presents detailed results for a single representative portfolio (the "Transportation" industry portfolio) in Panels A and B, and a summary of the results across all 30 industry portfolios in Panels C and D.

Panel A of Table 6 shows that the sup-t^2 test rejects the null of equal predictive accuracy, with p-values between 0.01 and 0.02. The ave-t^2 test has p-values around 0.075, indicating weaker evidence against the null of equal accuracy. The benchmark Diebold and Mariano (1995) test using the tick loss function fails to reject the null, with a p-value of 0.77. The one-sided sup-t test rejects the null, with p-values around 0.035, indicating that for some values of the elementary scoring rule parameter the RiskMetrics model is significantly better than the GARCH model, for some values of the loss parameter γ.

The upper panel of Figure 3 shows the "Murphy diagram" for this comparison, applied to the Transportation portfolio, and reveals that for most values of the elementary scoring rule parameter the GARCH and RiskMetrics forecasts have similar average losses. For values of the parameter around -1 the GARCH forecast significantly outperforms the RiskMetrics forecast, with the pointwise confidence intervals being far from zero, whereas the RiskMetrics forecast shows some (pointwise) significant outperformance for values of the parameter around -2.

Panel B of Table 6 compares the GARCH forecast with the rolling window sample quantile forecast. We find p-values for the tests of equal accuracy are zero to two decimal places, indicating strong evidence against this null. The one-sided test finds no evidence that the rolling window sample quantile outperforms the GARCH forecast for any value of elementary scoring rule parameter. The lower panel of Figure 3 shows that the difference in average loss is negative almost everywhere, consistent with the formal tests, and the pointwise confidence intervals exclude zero for a large part of the parameter space.

Panel C of Table 6 reports the proportion of the 30 industry portfolios for which we can reject the null at the 5% level. We see that the Diebold and Mariano (1995) test using the tick loss rejects the null of equal predictive accuracy for none of the 30 portfolios, while the ave-t^2 and sup-t^2 tests reject for around 23% and 10% of portfolios respectively. This suggests that the GARCH and RiskMetrics forecasts are generally not significantly different in terms of average loss, across the 30 industry portfolios. In contrast, Panel D shows that we can reject equal forecast accuracy of the GARCH and rolling window sample quantile forecasts for all 30 industry portfolios, and the one-sided sup-t test never finds significant evidence that the rolling window sample quantile outperforms the GARCH forecast for any part of the elementary scoring rule parameter space.

[Figure 3 about here.]

[Table 6 about here.]

6 Concluding remarks

In practical forecasting environments researchers are often faced with the problem of comparing forecasts using a loss function that contains a shape parameter; examples include comparisons using average utility across a range of values for the level of risk aversion, and comparisons using characteristics of a portfolio return across a range of values for the portfolio weight vector. We propose new forecast comparison tests, in the spirit of Diebold and Mariano (1995) and Giacomini and White (2006), that may be applied in such applications. We consider tests of the null of equal forecast accuracy across all values of the shape parameter, against the alternative of unequal forecast accuracy for some value of the shape parameter. We also consider one-sided tests for superior forecast accuracy. The asymptotic properties of the test statistics are derived using bootstrap theory for empirical processes, see Bühlmann (1995).

We show via an extensive simulation study that the tests have satisfactory finite-sample properties, unlike the leading existing alternatives which break down when a large number of values of the shape parameter is considered. We illustrate the new tests in three empirical applications: comparing portfolio strategies using average utility across a range of levels of risk aversion; comparing multivariate volatility models via their Value-at-Risk forecasts for portfolios of the underlying assets across a range of values for the portfolio weight vector; and comparisons using recently-proposed "Murphy diagrams' (Ehm et al., 2016) for classes of consistent scoring rules for quantile forecasting.

References

Andrews, D. W. (1992). Generic Uniform Convergence. *Econometric Theory*, 8(2):241–257.

Andrews, D. W. (1994). Chapter 37 Empirical Process Methods in Econometrics. volume 4 of *Handbook of Econometrics*, pages 2247–2294. Elsevier.

Bliss, R. R. and Panigirtzoglou, N. (2004). Option-Implied Risk Aversion Estimates. *The Journal of Finance*, 59(1):407–446.

Boussama, F., Fuchs, F., and Stelzer, R. (2011). Stationarity and Geometric Ergodicity of BEKK Multivariate GARCH Models. *Stochastic Processes and their Applications*, 121(10):2331–2360.

Bradley, R. C. et al. (2005). Basic Properties of Strong Mixing Conditions. A Survey and Some Open Questions. *Probability Surveys*, 2:107–144.

Bühlmann, P. (1995). The Blockwise Bootstrap for General Empirical Processes of Stationary Sequences. *Stochastic Processes and Their Applications*, 58(2):247–265.

Davydov, Y., Lifshits, M. A., and Smorodina, N. (1998). *Local Properties of Distributions of Stochastic Functionals*. American Mathematical Society.

DeMiguel, V., Garlappi, L., and Uppal, R. (2007). Optimal Versus equal weighted Diversification: How Inefficient is the 1/N Portfolio Strategy? *The Review of Financial Studies*, 22(5):1915–1953.

Diebold, F. X. and Mariano, R. S. (1995). Comparing Predictive Accuracy. *Journal of Business & Economic Statistics*, 13(3):253–263.

Doukhan, P., Massart, P., and Rio, E. (1994). The Functional Central Limit Theorem for Strongly Mixing Processes. In *Annales de l'IHP Probabilités et statistiques*, volume 30, pages 63–82. Gauthier-Villars.

Doukhan, P., Massart, P., and Rio, E. (1995). Invariance Principles for Absolutely Regular Empirical Processes. *Annales de l'I.H.P. Probabilités et Statistiques*, 31(2):393–427.

Ehm, W., Gneiting, T., Jordan, A., and Krüger, F. (2016). Of Quantiles and Expectiles: Consistent Scoring Functions, Choquet Representations and Forecast Rankings. *Journal of the Royal Statistical Society: Series B (Statistical Methodology)*, 78(3):505–562.

Engle, R. (2002). Dynamic Conditional Correlation: A Simple Class of Multivariate Generalized Autoregressive Conditional Heteroskedasticity Models. *Journal of Business & Economic Statistics*, 20(3):339–350.

Engle, R. and Colacito, R. (2006). Testing and Valuing Dynamic Correlations for Asset Allocation. *Journal of Business & Economic Statistics*, 24(2):238–253.

Fleming, J., Kirby, C., and Ostdiek, B. (2001). The Economic Value of Volatility Timing. *The Journal of Finance*, 56(1):329–352.

Fleming, J., Kirby, C., and Ostdiek, B. (2003). The Economic Value of Volatility Timing Using "Realized" Volatility. *Journal of Financial Economics*, 67(3):473–509.

Giacomini, R. and White, H. (2006). Tests of Conditional Predictive Ability. *Econometrica*, 74(6):1545–1578.

Gneiting, T. (2011a). Making and Evaluating Point Forecasts. *Journal of the American Statistical Association*, 106(494):746–762.

Gneiting, T. (2011b). Quantiles as Optimal Point Forecasts. *International Journal of Forecasting*, 27(2):197–207.

Hand, D. J. (1998). Data Mining: Statistics and More? *American Statistician*, 52(2):112–118.

Hansen, P. R. (2005). A test for superior predictive ability. *Journal of Business & Economic Statistics*, 23(4):365–380.

Kole, E., Markwat, T., Opschoor, A., and Van Dijk, D. (2017). Forecasting Value-at-Risk under Temporal and Portfolio Aggregation. *Journal of Financial Econometrics*, 15(4):649–677.

Kosorok, M. R. (2008). *Introduction to Empirical Processes and Semiparametric Inference*. Springer.

Kotz, S., Johnson, N. L., Balakrishnan, N., and Johnson, N. L. (2000). *Continuous Multivariate Distributions*. Wiley, New York.

Künsch, H. R. (1989). The Jackknife and the Bootstrap for General Stationary Observations. *The Annals of Statistics*, 17(3):1217–1241.

Marquering, W. and Verbeek, M. (2004). The Economic Value of Predicting Stock Index Returns and Volatility. *Journal of Financial and Quantitative Analysis*, 39(2):407–429.

McAleer, M. and Da Veiga, B. (2008). Single-Index and Portfolio Models for Forecasting Value-at-Risk Thresholds. *Journal of Forecasting*, 27(3):217–235.

Newey, W. K. and West, K. D. (1987). A Simple, Positive Semi-Definite, Heteroskedasticity and Autocorrelation Consistent Covariance Matrix. *Econometrica*, 55(3):703.

Riskmetrics (1996). JP Morgan Technical Document.

Santos, A. A., Nogales, F. J., and Ruiz, E. (2012). Comparing Univariate and Multivariate Models to Forecast Portfolio Value-at-Risk. *Journal of Financial Econometrics*, 11(2):400–441.

West, K. D. (1996). Asymptotic Inference about Predictive Ability. *Econometrica*, pages 1067–1084.

White, H. (2000). A Reality Check for Data Snooping. *Econometrica*, 68(5):1097–1126.

White, H. (2001). *Asymptotic Theory for Econometricians*. Academic Press, Cambridge, MA.

Wolak, F. A. (1987). An Exact Test for Multiple Inequality and Equality Constraints in the Linear Regression Model. *Journal of the American Statistical Association*, 82(399):782–793.

Wolak, F. A. (1989). Testing Inequality Constraints in Linear Econometric Models. *Journal of Econometrics*, 41(2):205–235.

Ziegel, J. F., Krüger, F., Jordan, A., and Fasciati, F. (2017). Murphy Diagrams: Forecast Evaluation of Expected Shortfall. *arXiv preprint arXiv:1705.04537*.

A Mathematical appendix

A.1 Proof of Theorem 1

Finite dimensional convergence of $\sqrt{n}\bar{L}_n(\cdot)$ follows from a CLT for (centered) stationary mixing sequences (e.g. Theorem 4 in Doukhan et al. (1994)), and the Crámer-Wold device (Proposition 5.1 in White (2001)), under Assumptions 1, 2, and 4. The mixing condition of Theorem 4 in Doukhan et al. (1994)) is satisfied if $\lim_{T\to\infty}\sum_{t=1}^{T} t^{1/(r-1)}\alpha(t) < \infty$. It is easy to see that this holds for $\alpha(t) = O(t^{-A})$, with $A > r/(r-1)$. Notice that β-mixing implies α-mixing, with relation $\alpha(t) \leq \frac{1}{2}\beta(t)$ between β-mixing and α-mixing coefficients (see, e.g., Doukhan et al. (1995, p. 397)). But under Assumption 1 $\beta(t)$ diminishes at a faster, geometric rate, such that the mixing condition is satisfied.

We apply Theorem 1 of Doukhan et al. (1995) to establish stochastic equicontinuity of $\sqrt{n}\bar{L}_n(\cdot)$.

First, notice from Application 1 in Doukhan et al. (1995) that the mixing condition is satisfied if $\lim_{T\to\infty}\sum_{t=1}^{T} t^{1/(r-1)}\beta(t) < \infty$, which was established in the preceding. Second, notice that under Assumption 2, the $L_{t+1}(\cdot)$ belong to $\mathcal{L}_{2r}$, where $\mathcal{L}_{2r}$ denotes the class of functions satisfying $\|f\|_{2r} < \infty$. From Application 1 in Doukhan et al. (1995) we then find that the entropy condition is satisfied if $\int_0^1 \sqrt{H_{[]}(\delta,\Gamma,\|\cdot\|_{2r})}du < \infty$, where $H_{[]}(\delta,\Gamma,\|\cdot\|_{2r})$ is defined as the natural logarithm of the $\mathcal{L}_{2r}$ bracketing numbers $N_{[]}(\delta,\Gamma,\|\cdot\|_{2r})$.

We can always choose N points in Γ, denoted γ_k, for $k = 1,\ldots,N$, and collected in Γ_N, such that for each $\gamma \in \Gamma$, $\min_k |\gamma - \gamma_k| < GN^{-1/d}$, because Γ is a bounded subset of $\mathbb{R}^d$.

Assumption 3 implies that $\|L_{t+1}(\gamma) - L_{t+1}(\gamma')\|_{2r} \le \|L_{t+1}(\gamma) - L_{t+1}(\gamma')\|_{4r} \le \bar{B}|\gamma - \gamma'|^{\lambda}$, for all $\gamma,\gamma' \in \Gamma$.

Setting $N(\delta) = \delta^{-d/\gamma}G^dB^{-d/\lambda}$, we therefore find that for all $\gamma \in \Gamma$ there exists a $\gamma_k \in \Gamma_N$ such that $\|L_{t+1}(\gamma) - L_{t+1}(\gamma_k)\|_{2r} \le B|\gamma - \gamma_k|^{\lambda} \le BG^{\lambda}N^{-\lambda/d} = \delta$. Hence, $N(\delta) = \delta^{-d/\lambda}G^d\bar{B}^{-d/\lambda}$ satisfies the definition of the $\mathcal{L}_{2r}$-bracketing numbers. Moreover, the entropy condition $\int_0^1 H_{[]}(\delta,\Gamma,\|\cdot\|_{2r})du = \int_0^1 \log(B^{d/\lambda}G^d\delta^{-d/\lambda})d\delta = d\log(B^{1/\lambda}G) + \int_0^1 \delta^{-d/\lambda}d\delta = d\log(B^{1/\lambda}G) + \frac{1}{2}\sqrt{\pi d/\lambda} < \infty$ holds.

It follows from Theorem 1 in Doukhan et al. (1995) that $\sqrt{n}\bar{L}_n(\cdot)$ is stochastically equicontinuous. Together with finite dimensional convergence this implies $\sqrt{n}\bar{L}_n(\cdot) \Rightarrow Z(\cdot)$, with $Z(\cdot)$ a Gaussian process with covariance kernel $\Sigma(\cdot,\cdot)$.

Note that $\sigma_n^2(\cdot) \xrightarrow{a.s} \sigma^2(\cdot)$ uniformly over Γ under Assumption 4. That $v(t_n) \xrightarrow{d} v(t_n)$ follows by application of the Continuous Mapping Theorem. □

A.2 Proof of Theorem 2

The result under H_0 follows from Theorem 1 and the distribution function of $v(\tilde{t})$ being absolutely continuous on $(0,\infty)$. The absolute continuity of the distribution function of $v(\tilde{t})$ follows from $Z(\cdot)$ having a nondegenerate covariance kernel, and thus $\tilde{t}(\cdot)$ having nondegenerate covariance kernel under Assumption 4, and the particular functional forms of $v(\cdot)$ under consideration (see Theorem 11.1 of Davydov et al. (1998)).

The result under H_1 is established as follows. Under the assumptions of Theorem 1 it follows that $\bar{L}_n(\gamma) \xrightarrow{a.s} E\left[L_{t+1}(\gamma)\right] \equiv \Delta(\gamma)$, uniformly over Γ.

Now notice that, for any $\gamma \in \Gamma$, $\left|E[L_{t+1}(\gamma^\dagger)]\right| - \left|E[L_{t+1}(\gamma^\dagger) - L_{t+1}(\gamma)]\right| \le \left|E[L_{t+1}(\gamma)]\right|$ by the Triangle Inequality. Furthermore, from Jensen's Inequality, Hölder's Inequality and under

Assumption 3, it follows that

$$\begin{aligned}\left|E[L_{t+1}(\gamma^\dagger) - L_{t+1}(\gamma)]\right| &\leq E\big[\left|L_{t+1}(\gamma^\dagger) - L_{t+1}(\gamma)\right|\big] \\ &\leq \left\|L_{t+1}(\gamma^\dagger) - L_{t+1}(\gamma)\right\|_{4r} \leq B|\gamma - \gamma^\dagger|^\lambda.\end{aligned}$$

Hence, if $\Gamma^\dagger = \{\gamma : |\gamma - \gamma'|^\lambda < \Delta/B\}$ has positive J-measure, there exists a $\Delta' > 0$ such that $|E[L_{t+1}(\gamma)]| = |\Delta(\gamma)| \geq \Delta'$, for all $\gamma \in \Gamma^\dagger$. It follows that $|\bar{L}_n(\gamma)| > \Delta'$, a.s., uniformly over $\Gamma^\dagger$.

Additionally, under Assumption 4 it follows that $\hat{\sigma}_n^2(\gamma) \xrightarrow{a.s.} \sigma_m^2(\gamma)$ uniformly over $\gamma \in \Gamma$, and $\inf_{\gamma\in\Gamma} \sigma^2(\gamma) > 0$, such that there exists a $\Delta'' > 0$ so that $n^{-1/2}|t_n(\gamma)| \xrightarrow{a.s.} n^{-1/2}\frac{|\bar{L}_n(\gamma)|}{\sigma(\gamma)} > \Delta''$, a.s., uniformly over $\Gamma^\dagger$. By application of the Continuous Mapping Theorem it follows that, a.s., $n^{-1}v(t_n^2) > 0$. Hence, $P[v(t_n^2) > c] \to 1$, for any constant $c \in \mathbb{R}$. □

A.3 Proof of Theorem 3

That $\sqrt{n}\bar{L}_n^*(\cdot) \Rightarrow Z(\cdot)$ almost surely follows from Theorem 1 in Bühlmann (1995). Assumption A1, A2, and A3 in Bühlmann (1995) are satisfied under Assumptions 1, 2, and 5 respectively. Finally, Assumption A4 in that paper is established in the proof of Theorem 1, since $N(\delta)$ satisfies the definition of the $\mathcal{L}_{4r}$ bracketing numbers, and $N(\delta) = \delta^{-d/\lambda}G^d\bar{B}^{-d/\lambda}$, for all $\delta > 0$.

Note that $\sigma_n^2(\cdot) \xrightarrow{a.s} \sigma^2(\cdot)$ uniformly over Γ under Assumption 4, such that $t_n^*(\cdot) \Rightarrow \tilde{t}(\cdot)$ almost surely under the Continuous Mapping Theorem.

That $v(t_n^*) \xrightarrow{d} v(t_n)$ in probability follows by application of a Continuous Mapping Theorem for bootstrapped processes (see Theorem 10.8 in Kosorok (2008)), given that the bootstrap is consistent in probability, which is implied by $\sqrt{n}\bar{L}_n^*(\cdot) \Rightarrow Z(\cdot)$ almost surely. The result follows.

□

A.4 Proof of Proposition 1

We show the result for $\text{ave}\, t_n^2$. The result for the other tests follows from similar steps. *Part 1:* The weak convergence of t_n^2 as established in Theorem 1 and the Continuous Mapping Theorem, implies stochastic equicontinuity (see, e.g., Proposition 1 in Andrews (1994)), i.e., for all $\varepsilon > 0$,

$$\lim_{\delta\downarrow 0} \limsup_{n\to\infty} P\left(\sup_{|\gamma-\gamma'|<\delta} \left|t_n^2(\gamma) - t_n^2(\gamma')\right| > \varepsilon\right) = 0,$$

where we again use the Euclidean metric to metrize Γ.

From absolute continuity of J it follows that that $\int_\Gamma dJ(\gamma) = \sum_{i=1}^{K_n} \int_{\Gamma_n^i} dJ(\gamma)$. Hence,

$$\begin{aligned}
&\left| \int_\Gamma t_n^2(\gamma) dJ(\gamma) - \sum_{i=1}^{K_n} t_n^2(\gamma_{n,i}) \int_{\Gamma_n^i} dJ(\gamma) \right| \\
&\quad \leq \sum_{i=1}^{K_n} \int_{\Gamma_n^i} \left| t_n^2(\gamma) - t_n^2(\gamma_{n,i}) \right| dJ(\gamma) \\
&\quad \leq \sum_{i=1}^{K_n} \sup_{\gamma \in \Gamma_n^i} \left| t_n^2(\gamma) - t_n^2(\gamma_{n,i}) \right| \int_{\Gamma_n^i} dJ(\gamma) \\
&\quad \leq \sup_{|\gamma - \gamma'| < \delta_n} \left| t_n^2(\gamma) - t_n^2(\gamma_{n,i}) \right| \sum_{i=1}^{K_n} \int_{\Gamma_n^i} dJ(\gamma) \\
&\quad = \sup_{|\gamma - \gamma'| < \delta_n} \left| t_n^2(\gamma) - t_n^2(\gamma_{n,i}) \right|,
\end{aligned}$$

For any $\varepsilon > 0$ there exists a $\delta > 0$ (with $\delta_n < \delta$ eventually), such that

$$\begin{aligned}
&\limsup_{n \to \infty} P\left(\left| \int_\Gamma t_n^2(\gamma) dJ(\gamma) - \sum_{i=1}^{K_n} t_n^2(\gamma_{n,i}) \int_{\Gamma_n^i} dJ(\gamma) \right| > \varepsilon' \right) \\
&\quad \leq \limsup_{n \to \infty} P\left(\sup_{|\gamma - \gamma'| < \delta_n} \left| t_n^2(\gamma) - t_n^2(\gamma_{n,i}) \right| > \varepsilon \right) \\
&\quad \leq \limsup_{n \to \infty} P\left(\sup_{|\gamma - \gamma'| < \delta} \left| t_n^2(\gamma) - t_n^2(\gamma_{n,i}) \right| > \varepsilon \right) < \varepsilon,
\end{aligned}$$

where the last display follows from the stochastic equicontinuity of $t_n^2(\gamma)$. Because δ is arbitrary, the result follows.

Part 2: We cover Γ with some hyperrectangle $\bar{\Gamma}$, which we can do because Γ is a bounded subset of Euclidian space. Consider the d-dimensional hyperrectangular grid of $\bar{\Gamma}$ with $\bar{K}_n$ elements $\{\bar{\Gamma}_n^i\}_{i=1}^{\bar{K}_n}$, such that $\sup_{\gamma, \gamma' \in \bar{\Gamma}_n^i} |\gamma - \gamma'| < \delta_n$, for all $i = 1, \ldots, \bar{K}_n$.

Now let $\{\Gamma_i^n\}_{i=1}^{K_n}$ be the K_n elements of $\{\bar{\Gamma}_n^i\}_{i=1}^{\bar{K}_n}$, such that $\Gamma_i^n \cap \Gamma$ is nonempty, and choose the $\gamma_{n,i}$ such that $\gamma_{n,i} \in \Gamma$.

We can expand

$$\begin{aligned}
&\widetilde{\operatorname{ave} t_n^2} - \widehat{\operatorname{ave} t_n^2} \\
&\quad = \frac{1}{S_n}\sum_{j=1}^{S_n} t_n^2(\gamma^{(j)}) - \sum_{i=1}^{K_n} t_n^2(\gamma_{n,i}) \int_{\Gamma_n^i} dJ(\gamma) \\
&\quad = \sum_{i=1}^{K_n} t_n^2(\gamma_{n,i}) \left\{ \frac{1}{S_n}\sum_{j=1}^{S_n} \mathbb{1}\left(\gamma^{(j)} \in \Gamma_i^n\right) - \int_{\Gamma_n^i} dJ(\gamma) \right\} \\
&\qquad + \sum_{i=1}^{K_n} \frac{1}{S_n}\sum_{j=1}^{S_n} \left(t_n^2(\gamma^{(j)}) - t_n^2(\gamma_{n,i}) \right) \mathbb{1}\left(\gamma^{(j)} \in \Gamma_i^n\right) \\
&\quad = A_n + B_n.
\end{aligned}$$

Notice that

$$\begin{aligned}
|A_n| &\le \sup_{\gamma\in\Gamma} t_n^2(\gamma) \cdot \sum_{i=1}^{K_n} \Big| \frac{1}{S_n}\sum_{j=1}^{S_n} \mathbb{1}\Big(\gamma^{(j)} \in \Gamma_i^n\Big) - \int_{\Gamma_n^i} dJ(\gamma) \Big| \\
&\le K_n \sup_{\gamma\in\Gamma} t_n^2(\gamma) \sup_{\Gamma'\subset\Gamma} \Big| \frac{1}{S_n}\sum_{j=1}^{S_n} \mathbb{1}\Big(\gamma^{(j)} \in \Gamma'\Big) - \int_{\Gamma'} dJ(\gamma) \Big| \\
&= K_n O_p(1) C_n,
\end{aligned}$$

where the last line follows from Theorem 1.

Furthermore, we can show that $S_n^{1/2-\eta} C_n = o_p(1)$, for any $\eta \in (0, 1/2)$, where the probability statement now holds under the J-measure, by a CLT for iid empirical processes. Notice that due to the hyperrectangular shape of the Γ_i^n, we have for each $\Gamma_i^n \subset \bar{\Gamma}$

$$\mathbb{1}\left(\gamma \in \Gamma_i^n\right) = \prod_{i=1}^{d} \mathbb{1}\left(\gamma_i \le \overline{\gamma_i^n}\right) \prod_{i=1}^{d} \Big(1 - \mathbb{1}\Big(\gamma_i \le \underline{\gamma_i^n}\Big)\Big), \tag{41}$$

with $\bar{\gamma}_i^n$ denotes the maximum of the ith coordinate of all points in Γ_i^n, and with $\underline{\gamma_i^n}$ denoting the mininum.

Indicator functions such as the factors in (41) are type I(b) functions in the definition of Andrews (1994), and by Theorem 3 in Andrews (1994) so is the product (41). A functional CLT follows from Theorem 1 and 2 in Andrews (1994)), and by application of the Continuous Mapping Theorem we find $\sup_{\Gamma'\subset\bar{\Gamma}} \left| \frac{1}{S_n}\sum_{j=1}^{S_n} \mathbb{1}\left(\gamma^{(j)} \in \Gamma'\right) - \int_{\Gamma'} dJ(\gamma) \right| = O_p(S_n^{-1/2})$. Hence, $S_n^{1/2-\eta} C_n = O_p(1)$.

Furthermore, notice that

$$
\begin{aligned}
|B_n| &\leq \frac{1}{S_n} \sum_{j=1}^{S_n} \sum_{i=1}^{K_n} \left| t_n^2(\gamma^{(j)}) - t_n^2(\gamma_{n,i}) \right| \mathbb{1}\left(\gamma^{(j)} \in \Gamma_i^n \right) \\
&\leq 2^d \frac{1}{S_n} \sum_{j=1}^{S_n} \sup_{|\gamma^{(j)} - \gamma'| < \delta_n} \left| t_n^2(\gamma^{(j)}) - t_n^2(\gamma') \right| \\
&\leq 2^d \sup_{|\gamma - \gamma'| < \delta_n} \left| t_n^2(\gamma) - t_n^2(\gamma') \right| = o_p(1),
\end{aligned}
$$

by the stochastic equicontinuity of $t_n^2(\gamma)$ and where 2^d equals the maximum number of vertices shared amongst hyperrectangles in a hyperrectangular grid.

If we can choose $K_n = o(S_n^{-1/2+\eta})$ then $|A_n| = O_p(1)K_nC_n = O_p(1)o_p(1) = o_p(1)$. Hence, $|\widetilde{\text{ave}\, t_n^2} - \widehat{\text{ave}\, t_n^2}| = o_p(1)$. But we are free to choose the rate at which $K_n \to \infty$ as $n \to \infty$, so the result follows.

□

Table 1: Small sample rejection rates of equal expected utility tests on equal weighted and minimum-variance portfolio strategies

	2-sided tests				1-sided tests	
K_n	Wald	Bonferroni	ave-t^2	sup-t^2	Bonferroni	sup-t
Panel A: Size properties						
				n = 120		
1	0.14	0.14	0.13	0.13	0.17	0.19
10	0.58	0.06	0.09	0.12	0.07	0.15
50	0.50	0.04	0.08	0.14	0.04	0.16
100	0.50	0.04	0.09	0.14	0.05	0.18
250	-	0.03	0.09	0.13	0.04	0.17
				n = 600		
1	0.06	0.06	0.06	0.06	0.07	0.08
10	0.48	0.02	0.04	0.06	0.02	0.07
50	0.50	0.01	0.06	0.07	0.01	0.10
100	0.50	0.01	0.06	0.08	0.01	0.10
250	0.51	0.00	0.05	0.07	0.01	0.08
Panel B: Power properties						
				n = 120		
1	0.12	0.12	0.12	0.12	0.01	0.01
10	0.98	0.81	0.47	0.94	0.86	0.96
50	0.53	0.65	0.41	0.92	0.70	0.96
100	0.29	0.61	0.40	0.93	0.67	0.96
250	-	0.51	0.40	0.94	0.57	0.95
				n = 600		
1	0.76	0.76	0.77	0.77	0.00	0.00
10	0.99	1.00	1.00	1.00	1.00	1.00
50	0.80	1.00	1.00	1.00	1.00	1.00
100	0.67	1.00	1.00	1.00	1.00	1.00
250	0.51	1.00	1.00	1.00	1.00	1.00

Note: This table presents p-values of the one-sided and two-sided tests as well as the benchmark tests. The data is generated according to Equation (30), and the equal-weighed and minimum-variance portfolio strategies are given in Equation (29). The minimum-variance portfolio weights are estimated using a rolling window of $m = 120$ observations. The out-of-sample period consists of $n = 120$, and 600 observations. We consider discrete grids of $\Gamma = [1, 10]$ with $K_n = 1, 10, 50, 100,$ and 250 equally spaced grid points. Results for the multivariate Wald test with $K_n = 250$ are not shown for $n = 120$, due to the singularity of the covariance matrix.

Table 2: Small sample rejection rates of quantile forecast tests, for differences between multivariate GARCH-DCC and RiskMetrics models

	2-sided tests				1-sided tests	
S_n	Wald	Bonferroni	ave-t^2	sup-t^2	Bonferroni	sup-t
Panel A: Size properties						
				n = 500		
31	0.36	0.03	0.03	0.05	0.01	0.01
50	0.93	0.03	0.03	0.04	0.01	0.01
100	1.00	0.02	0.03	0.04	0.00	0.01
250	1.00	0.01	0.03	0.04	0.00	0.01
500	-	0.01	0.03	0.04	0.00	0.01
1000	-	0.01	0.03	0.05	0.00	0.01
				n = 2,000		
31	0.03	0.01	0.01	0.02	0.01	0.01
50	0.13	0.01	0.02	0.01	0.00	0.01
100	0.81	0.00	0.01	0.01	0.00	0.01
250	1.00	0.00	0.02	0.01	0.00	0.01
500	1.00	0.00	0.02	0.01	0.00	0.01
1000	1.00	0.00	0.02	0.01	0.00	0.01
Panel B: Power properties						
				n = 500		
31	0.42	0.10	0.20	0.11	0.16	0.15
50	0.91	0.07	0.16	0.10	0.11	0.14
100	1.00	0.05	0.13	0.10	0.07	0.14
250	1.00	0.03	0.11	0.10	0.04	0.14
500	-	0.02	0.12	0.10	0.03	0.14
1000	-	0.01	0.11	0.10	0.02	0.13
				n = 2,000		
31	0.33	0.50	0.81	0.52	0.62	0.65
50	0.38	0.42	0.66	0.52	0.55	0.64
100	0.82	0.30	0.52	0.50	0.43	0.63
250	1.00	0.20	0.46	0.50	0.28	0.64
500	1.00	0.14	0.46	0.51	0.21	0.64
1000	1.00	0.09	0.43	0.49	0.15	0.64

Note: This table presents rejection rates of the one-sided and two-sided tests as well as the benchmark tests in our size and power experiments. The quantile forecasts for the portfolio returns from the GARCH-DCC and multivariate RiskMetrics models are defined in Equations (32) and Equation (33), respectively. The data is generated as in Equation (31) with $N = 30$. We let Γ be the set of all portfolio weight vectors with positive portfolio weights summing to one. We test at 31 fixed portfolio weight vector being the equal weighted portfolio vector and the 30 basis vectors, as well as $S_n - 31$ weight vectors drawn uniformly from Γ, with $S_n = 50, 100, 250, 500$, and 1,000.

Table 3: Small sample rejection rates of Murphy diagram tests, for quantile forecast differences between GARCH and RiskMetrics models

	2-sided tests			1-sided tests	
K_n	tick-loss	ave-t^2	sup-t^2	tick-loss	sup-t
Panel A: Size properties, GARCH vs RiskMetrics					
			n = 500		
1	0.07	-	-	0.04	-
50	-	0.04	0.04	-	0.03
100	-	0.03	0.03	-	0.02
250	-	0.02	0.02	-	0.01
			n = 2,000		
1	0.06	-	-	0.04	-
50	-	0.04	0.05	-	0.03
100	-	0.05	0.05	-	0.04
250	-	0.04	0.04	-	0.04
Panel B: Size properties, GARCH vs 250-day rolling window sample quantile					
			n = 500		
1	0.21	-	-	0.05	
50	-	0.14	0.12	-	0.07
100	-	0.14	0.10	-	0.09
250	-	0.15	0.09	-	0.08
			n = 2,000		
1	0.16	-	-	0.06	-
50	-	0.11	0.08	-	0.05
100	-	0.13	0.09	-	0.08
250	-	0.14	0.07	-	0.06
Panel C: Power properties, GARCH vs RiskMetrics					
			n = 500		
1	0.11	-	-	0.19	-
50	-	0.04	0.04	-	0.06
100	-	0.04	0.04	-	0.06
250	-	0.03	0.03	-	0.04
			n = 2,000		
1	0.37	-	-	0.49	-
50	-	0.10	0.08	-	0.14
100	-	0.10	0.08	-	0.13
250	-	0.12	0.10	-	0.15
Panel D: Power properties, GARCH vs 250-day rolling window sample quantile					
			n = 500		
1	0.32	-	-	0.45	-
50	-	0.26	0.27	-	0.36
100	-	0.33	0.30	-	0.39
250	-	0.30	0.27	-	0.36
			n = 2,000		
1	0.90	-	-	0.95	-
50	-	0.76	0.72	-	0.81
100	-	0.85	0.77	-	0.85
250	-	0.89	0.82	-	0.88

Note: This table presents rejection rates of the one-sided and two-sided tests as well as the benchmark tests using the tick-loss function in our size and power experiments. The quantile forecasts from the GARCH and RiskMetrics models are given in Equations (32) and Equation (33), respectively, with $N = 1$. We consider out-of-sample period lengths n = 500, and 2,000, and discrete grids of $\Gamma = [-20, 0]$ with $K_n = 50, 100$, and 250 equally spaced grid points. The tick-loss based tests use only a single loss function, and are reported in the rows labeled $K_n = 1$.

Table 4: p-values from tests of equal expected utility from equal weighted and minimum-variance portfolio strategies

	2-sided tests				1-sided tests	
K_n	Wald	Bonferroni	ave-t^2	sup-t^2	Bonferroni	sup-t
Panel A: $\Gamma = [1, 10]$						
1	0.03	0.03	0.04	0.04	0.02	0.01
10	0.00	0.04	0.13	0.01	0.02	0.00
50	0.00	0.22	0.17	0.01	0.11	0.00
100	0.00	0.45	0.16	0.01	0.22	0.00
250	0.26	1.00	0.16	0.02	0.56	0.01
Panel B: $\Gamma = [1, 5]$						
1	0.03	0.03	0.04	0.04	0.02	0.02
10	0.00	0.04	0.07	0.01	0.02	0.00
50	0.00	0.22	0.07	0.01	0.11	0.00
100	0.00	0.45	0.06	0.01	0.22	0.00
250	0.00	1.00	0.04	0.01	0.56	0.01
Panel C: $\Gamma = [5, 10]$						
1	0.87	0.87	0.87	0.87	0.56	0.57
10	0.00	1.00	0.53	0.38	1.00	0.22
50	0.00	1.00	0.53	0.36	1.00	0.17
100	0.00	1.00	0.62	0.41	1.00	0.22
250	0.02	1.00	0.58	0.38	1.00	0.20

Note: This table presents rejection rates of the one-sided and two-sided tests as well as the benchmark tests in our size and power experiments. The equal weighted and minimum-variance portfolio strategies are given in Equation (29). The data consists of monthly returns of 30 industry portfolios and runs from September 1926 to December 2017. We consider risk aversion parameters in the range $\Gamma = [1, 10]$ (upper panel), $\Gamma = [1, 5]$ (middle panel), and $\Gamma = [5, 10]$ (lower panel). $K_n = 1, 10, 50, 100$, and 250 indicates the number of (equally-spaced) grid points. The one-sided tests examine whether the equal weighted portfolio outperforms the minimum-variance portfolio.

Table 5: p-values of quantile forecast tests, for differences between multivariate GARCH-DCC and RiskMetrics models

	2-sided tests				1-sided tests	
S_n	Wald	Bonferroni	ave-t^2	sup-t^2	Bonferroni	sup-t
Panel A: Full sample						
1	0.78	0.78	0.79	0.79	0.39	0.39
31	0.99	1.00	0.99	0.95	1.00	0.62
100	-	1.00	0.94	0.95	1.00	0.64
250	-	1.00	0.81	0.93	1.00	0.59
500	-	1.00	0.79	0.90	1.00	0.54
1000	-	1.00	0.74	0.90	1.00	0.58
Panel B: First sub-sample						
1	0.30	0.30	0.30	0.30	0.15	0.15
31	0.01	0.05	0.04	0.04	0.02	0.02
100	-	0.16	0.22	0.05	0.08	0.03
250	-	0.40	0.23	0.05	0.20	0.03
500	-	0.80	0.24	0.06	0.40	0.04
1000	-	1.00	0.23	0.05	0.80	0.03
Panel C: Second sub-sample						
1	0.32	0.32	0.34	0.34	0.84	0.85
31	0.33	0.35	0.22	0.17	1.00	0.87
100	-	1.00	0.28	0.16	1.00	0.90
250	-	1.00	0.28	0.18	1.00	0.91
500	-	1.00	0.30	0.18	1.00	0.90
1000	-	1.00	0.30	0.17	1.00	0.91

This table presents p-values of the one-sided and two-sided tests as well as the benchmark tests. The quantile forecasts for the portfolio returns from the GARCH-DCC and multivariate RiskMetrics models are defined in Equations (32) and Equation (33), respectively. The data consists of twenty years of daily returns of 30 industry portfolios and runs from January 1998 to December 2017. We let Γ be the set of all portfolio weight vectors with positive portfolio weights summing to one. We test at 31 fixed portfolio weight vector being the equal weighted portfolio vector and the 30 basis vectors, as well as $S_n - 31$ weight vectors drawn uniformly from Γ, with $S_n = 100, 250, 500,$ and 1,000. The one-sided tests examine whether the GARCH-DCC forecast is outperformed by the RiskMetrics forecast.

Table 6: Quantile forecast comparison tests, for the Transportation industry portfolio and across all 30 industry portfolios.

	2-sided tests			1-sided tests	
K_n	tick-loss	ave-t^2	sup-t^2	tick-loss	sup-t
Panel A: p-values for Transportation portfolio, RiskMetrics vs. GARCH					
1	0.77	-	-	0.38	-
50	-	0.02	0.00	-	0.01
100	-	0.07	0.01	-	0.04
250	-	0.08	0.02	-	0.04
500	-	0.07	0.01	-	0.03
1000	-	0.08	0.02	-	0.04
Panel B: p-values for Transportation portfolio, rolling window vs. GARCH					
1	0.00	-	-	0.00	-
50	-	0.00	0.00	-	0.96
100	-	0.00	0.00	-	0.98
250	-	0.00	0.00	-	0.99
500	-	0.00	0.00	-	0.98
1000	-	0.00	0.00	-	0.99
Panel C: Rejection proportions over 30 industry portfolios, RiskMetrics vs. GARCH					
1	0.00	-	-	0.00	-
50	-	0.07	0.07	-	0.13
100	-	0.30	0.17	-	0.23
250	-	0.20	0.07	-	0.13
500	-	0.23	0.10	-	0.20
1000	-	0.23	0.10	-	0.10
Panel D: Rejection proportions over 30 industry portfolios, rolling window vs. GARCH					
1	1.00	-	-	0.00	-
50	-	1.00	1.00	-	0.00
100	-	1.00	1.00	-	0.00
250	-	1.00	1.00	-	0.00
500	-	1.00	1.00	-	0.00
1000	-	1.00	1.00	-	0.00

Note: This table presents results comparing the accuracy of forecasts of the 5% quantile for daily returns of 30 industry portfolios, as generated by univariate GARCH and RiskMetrics models. Panels A and B present p-values from one-sided and two-sided tests based on the elementary scoring rules for the quantile, as well as benchmark tests using the tick-loss function, applied to daily returns on the Transportation industry portfolio. Panels C and D report proportions of rejections, at the 5% significance level, across all 30 industry portfolios. We consider equally-spaced discrete grids of $\Gamma = [-20, 0]$ with $K_n = 50, 100, 250, 500$ and 1000. The tick-loss based tests use only a single loss function, and are reported in the rows labeled $K_n = 1$. The data runs from January 1998 to December 2017. The one-sided tests examine whether the GARCH forecast is outperformed by the RiskMetrics or rolling window sample quantile forecasts.

Figure 1: Utility differential of equal weighted and minimum-variance portfolio strategies

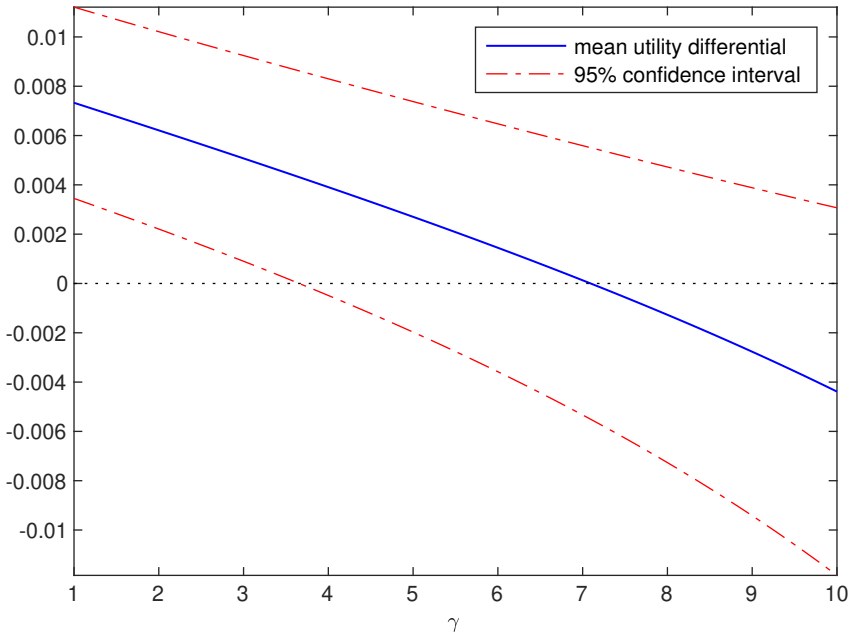

Note: This figure plots the the sample mean of utility derived from the equal weighted portfolio strategy *minus* the sample mean of utility derived from the minimum-variance portfolio strategies. The strategies are given Equation (29). The data consists of monthly returns of 30 industry portfolios and runs from September 1926 to December 2017. We consider risk aversion parameters in the range $\Gamma = [1, 10]$.

Figure 2: Tick-loss differential for tail quantile forecasts generated by the multivariate GARCH-DCC and RiskMetrics models

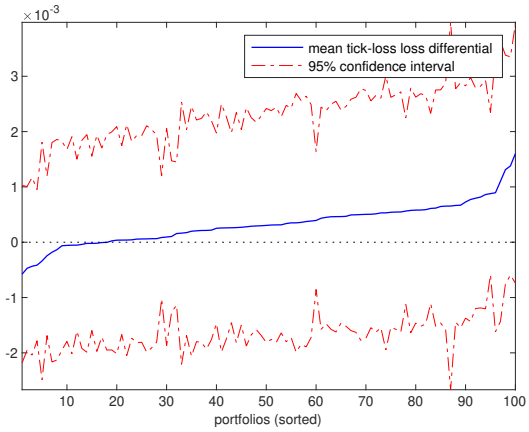

(a) Full sample

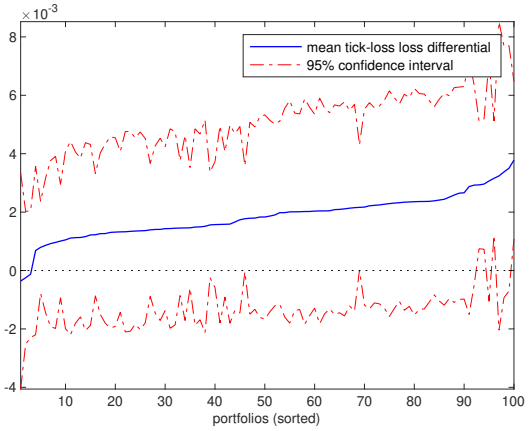

(b) First half of sample

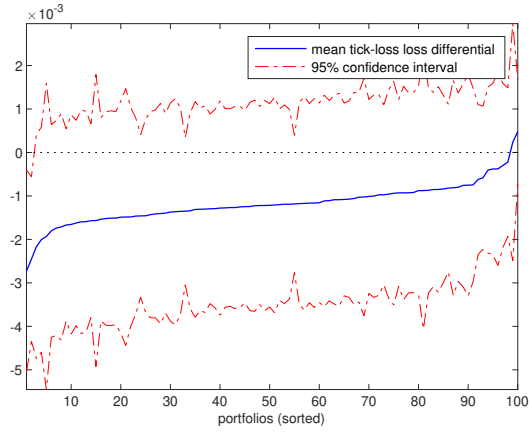

(c) Second half of sample

Note: This figure plots the sample mean tick-loss of the GARCH-DCC forecasts *minus* the sample mean tick-loss of the RiskMetrics forecasts. The forecasts are defined in Equations (32) and Equation (33). The mean tick-loss differences are shown for the first $S_n = 100$ portfolio weight vectors and sorted on mean tick-loss difference. The first 31 portfolio weight vectors are the equal weighted portfolio vector and the 30 single-asset portfolio vectors. The 69 additional portfolio vectors are drawn uniformly from Γ, the 30-dimensional simplex. The data consists of daily returns for 30 Industry portfolios and runs from January 1998 to December 2017.

Figure 3: Murphy diagrams; elementary loss differential between quantile forecasts for the Transportation portfolio

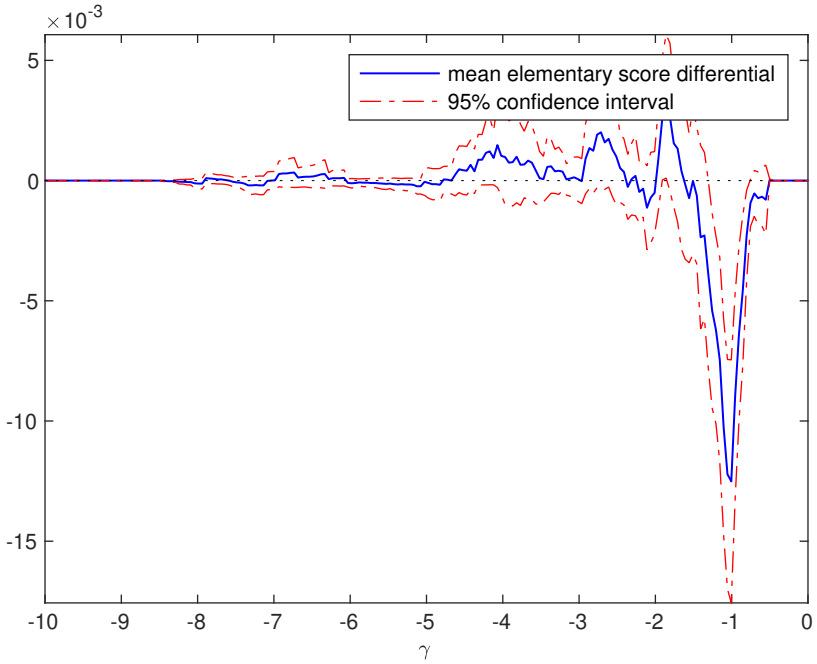

(a) GARCH vs. RiskMetrics

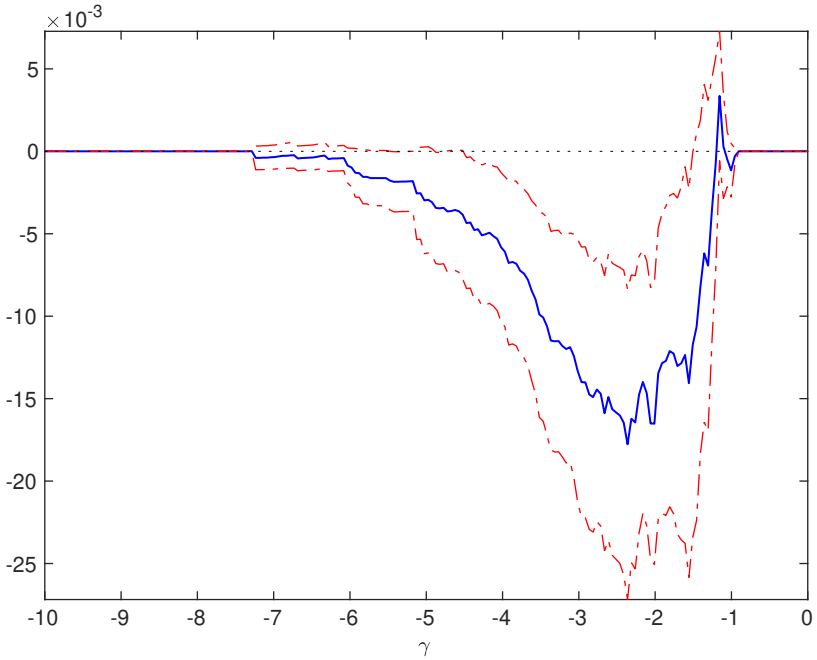

(b) GARCH vs. rolling window sample quantile

Note: This figure plots the sample mean of the elementary scoring rule of the GARCH forecasts *minus* the sample mean of the elementary scoring rule of the RiskMetrics forecasts. The forecasts under consideration are 5% quantile forecasts for daily returns of the US Transportation industry index. The elementary scoring rules are indexed by scalar parameter γ on $\Gamma = [-10, 0]$. The data consists of daily returns of 30 Industry portfolios and runs from January 1998 to December 2017.